RESEARCH

Multi-component Adsorption Isotherms: Review and Modeling Studies

Amrutha[1] · Gautham Jeppu[1] · C. R. Girish[1] · Balakrishna Prabhu[1] · Katharina Mayer[2]

Abstract

Adsorption is an important phenomenon widely used for the removal of contaminants. Several drinking water contaminants such as arsenic and fluoride, vanadium and chromium, nickel, cadmium and cobalt are found to coexist in nature as multi-component mixtures in water. Hence, the modeling of multi-component adsorption isotherms for designing water treatment systems has gained importance recently. However, review studies of multi-component adsorption and competitive adsorption modeling are limited. The current review paper summarizes twenty-six multi-component adsorption isotherm models. Also, case studies of several common multi-component adsorption systems and the mechanisms of multi-component adsorption are discussed. Furthermore, a modeling analysis of four multi-component isotherms models for three commonly found two-component adsorption systems, i.e., cadmium-nickel, nickel–cobalt, and cadmium-cobalt, is reported. The Extended Langmuir isotherm, Competitive Langmuir isotherm, Extended Langmuir–Freundlich isotherm and Extended Freundlich isotherm models were applied in the modeling study for the competitive adsorption of Cd, Ni, and Co. The goodness of fit parameters and adsorption isotherm constants were estimated for these models. The factors influencing competitive adsorption, mechanisms of adsorption, various single and multi-component isotherm models, their significance, and limitations are also discussed in this review article.

Highlights

• Twenty-six multi-component and ten single-component isotherm models are compiled
• Factors affecting multi-component competitive adsorption isotherms are discussed in this review paper
• The applications of four multi-component isotherm models for three binary contaminant systems are presented.

✉ Gautham Jeppu
  gautham.jeppu@gmail.com

✉ C. R. Girish
  girishcrtd@gmail.com

1 Department of Chemical Engineering, Manipal Institute of Technology (MIT), Manipal Academy of Higher Education (MAHE), Manipal 576104, Karnataka, India

2 Department of Chemical and Process Engineering, Technical University of Vienna, Karlsplatz, Vienna, Austria

1 Introduction

The quality of the water is decreasing as environmental contamination rises. Water pollution is caused by heavy metals, stormwater, sewage water, radioactive materials, and treated wastewater discharges from industries into rivers and the oceans (DhanaRamalakshmi et al. 2020; Janani et al. 2022; Say et al. 2003). Insecticides, toxic chemicals, heavy metal ions, radioactive nuclides, and other substances that are toxic to living beings are also frequent water contaminants (Puri et al. 2021). According to Lakherwal (2019), hazardous chemicals in water can harm the skin, brain, stomach, nervous system, heart, blood flow, bones, and kidney. Additionally, they may cause respiratory illness, mental retardation, nausea, exhaustion, thyroid dysfunction, elevated blood pressure, joint discomfort, tooth discoloration, anemia, blindness, and hearing. Water pollution also impacts the immunological and reproductive systems (Foo and Hameed 2010).

Many technologies are used for water treatment, including reverse osmosis, electrodialysis, membrane separation, filtration, coagulation, precipitation, and adsorption (He et al. 2020). Adsorption is the most feasible and commonly used method due to its ease of use. The major water purification systems are based on adsorption phenomena. Since German physicist Heinrich Kayser first used the word in 1881, adsorption has been thoroughly studied. The adsorption technique has since been widely used because of its simplicity and low cost (Rathore et al. 2016).

The adsorption process occurs through physical or chemical linkages between the adsorbent and the adsorbate. Adsorption is now highly relevant and valuable in the contemporary environment. It is utilized in several industrial processes, including wastewater treatment, flue gas stream purification, air pollution masks, heterogeneous catalysis, various chromatography methods, and many more (Bibi et al. 2015). Although single-component adsorption has been the subject of extensive research, most adsorption applications involve systems with multiple components. For example, arsenic and fluoride are found together in many places in India, China, Mexico, Japan and the USA. Lead and zinc, vanadium and chromium, zinc and nickel, cobalt and nickel and many other contaminants occur simultaneously in the sediments and unconfined aquifers leading to contamination of groundwater. Industrial wastewater usually consists of several pollutants such as lithium, phosphorus, chromium, nickel, cadmium, cobalt, copper, mercury along with other organic pollutants. These pollutants also interact with each other and may show synergistic or antagonistic behavior during adsorption. However, there are only few conclusive multi-component adsorption modeling studies for adsorption of such mixtures.

The adsorption of contaminants may be done using several adsorbents, including activated carbon, zeolites, iron oxides, alumina, silica gel, and nanoparticles (Dhanasekaran and Sahu 2021). Materials such as biochar, agricultural wastes, modified sawdust, and activated alumina are commonly used for column studies. Also, activated carbon derived from various readily available materials, industrial-based materials such as iron oxide, manganese oxide, iron-coated sand (Jeppu et al. 2010), and ferric hydroxide with iron oxide are widely used for water treatment (Bibi et al. 2017).

Adsorption modeling studies are essential for research of the adsorption process (Abdoul Magid et al. 2021; Wang et al. 2017). The strength, maximum adsorption capacity, and

adsorption affinity of the adsorbent system are quantified and provided through isotherm modeling. Adsorption isotherms give information on the adsorbent material's nature, including its surface area, pore size distribution, and the potency of adsorbent-adsorbate interactions. The performance of the materials in various applications, including catalysts, water filtration, and gas storage, may be predicted using this knowledge. Adsorption isotherms may be used to identify the ideal operating conditions for an adsorption process, including the temperature, pressure, and adsorbate concentration which aids in maximizing process effectiveness and lowering costs. Adsorption isotherm models may create adsorption systems tailored to a particular purpose. For instance, the models can predict the quantity of adsorbent needed to treat a specific volume of gas or liquid. Adsorption isotherms may be used to check the quality of adsorbent materials. The performance of the material under various situations may be predicted using the models, and the performances of multiple adsorbents can be compared. Adsorption isotherm modeling, in general, is a crucial tool for comprehending and improving, and assessing adsorption systems for several applications.

Modern research in multi-component or competitive adsorption still needs to advance, especially in comparison to the work done in single-component adsorption. A thorough interpretation of the isotherm models would significantly improve the competitive adsorption isotherm modeling (Ashour et al. 2022). Research on the simultaneous removal of dangerous contaminants by several adsorbents has recently been conducted (Adamu et al. 2018). In order to improve the design of the adsorbents and the adsorption system pattern, it is imperative and trustworthy to study the multi-component adsorption process (Chen et al. 2022b; Van Assche et al. 2018).

It should be easier to assess competing adsorption isotherm models thoroughly. There are limitations to the compilation of all multi-component isotherm models. However, their use is beneficial and practical (Qiao and Hu 2000). Adsorption considerations include temperature, pH, concentration, and how the adsorbent and adsorbate interact (Musso et al. 2019). Single-component systems are easier to model and implement than multi-component systems. Adsorption equilibrium conditions, the interaction coefficient between adsorbates and adsorbents, and the adsorbate distribution coefficient are a few of the numerous variables in multi-component adsorption systems. Affinity parameter of adsorption, non-interaction between adsorbents and adsorbates (Weerasundara et al. 2021; Wu et al. 2012), optimum adsorption capacity, selection of adsorbent for specific adsorbate, and antagonistic and synergetic behavior of adsorption are also included (Girish 2018). Adsorption models are nonlinear and multivariable, mainly when analyzing multi-component systems (groundwater, industrial effluents, and wastewater). As a result, adsorption data modeling is a complex mathematical issue requiring a nonlinear data regression process for determining model parameters with a correct error function and a thorough statistical analysis to determine model performance (Sellaoui et al. 2018).

The Scopus search engine was utilized in the literature search to retrieve published articles in the many subject areas. The search terms for the survey were adsorption, mono-component adsorption, and single-component adsorption isotherm models. A total of 20,894 scientific articles on adsorption were produced between 1986 and 2023. The disciplines with the highest levels of research include environmental science, chemistry, chemical engineering, engineering, and material science. A good number of papers have been written regarding single-component adsorption and multi-component adsorption (Figs. 1, 2 and 3).

Competitive adsorption or multi-component adsorption isotherm models are the search terms utilized in the survey. Between 1986 and 2023, only 401 research publications were published on multi-component isotherm models, showing fewer studies on multi-component adsorption. Most relevant publications are used in chemistry, environmental science, chemical
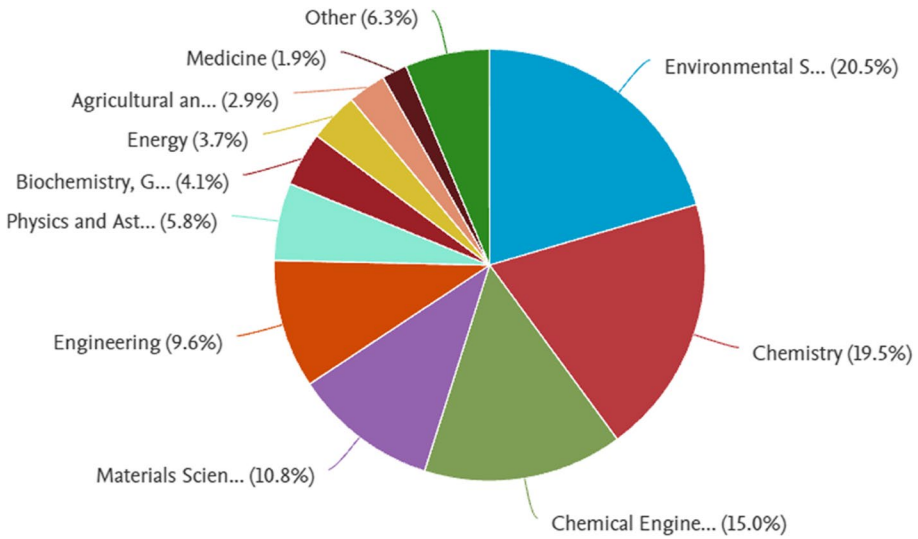
Fig. 1 Trend of publication of mono-component adsorption in various research areas as per Scopus

engineering, engineering, and material science, demonstrating the need for this review. Therefore, there is a strong and increasing need for research on competitive adsorption. Due to a lack of literature on review of competitive adsorption models, a collection of isotherm models of competitive adsorption has become essential.

Between 1986 and 2023, nearly 357 research articles were published on multi-component adsorption. The search keywords used in this study are taken from the Scopus tool: competitive adsorption modeling, multi-component adsorption isotherm models, or competitive adsorption isotherm models. The acceptable subjects of study are chemistry, environmental science, chemical engineering, biochemistry, and engineering. It is essential to have adequate
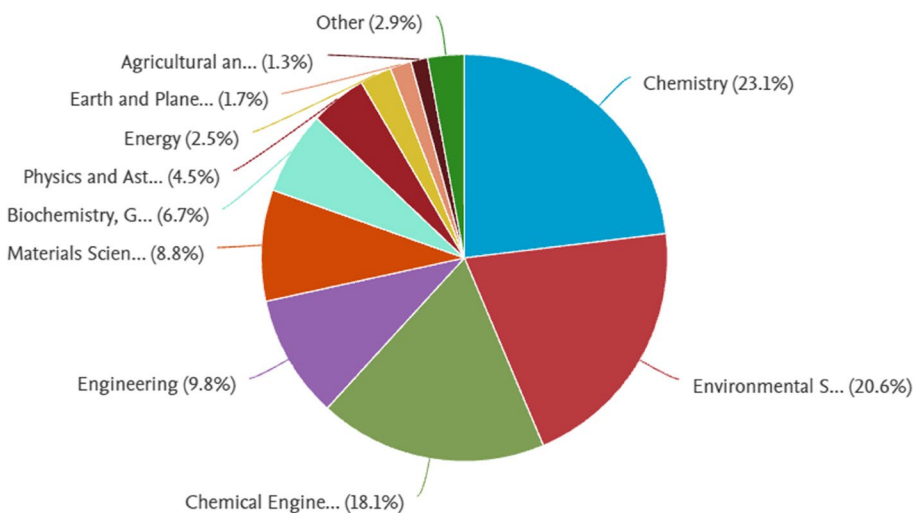

Fig. 2 Trend of publication of multi-component adsorption in various research areas as per Scopus
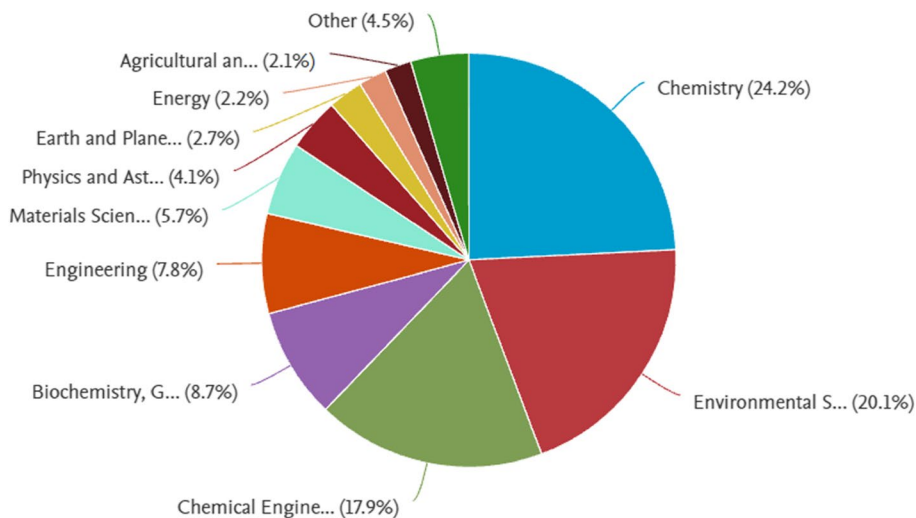
Fig. 3 Trend of publication of multi-component adsorption modeling in various research areas as per Scopus

literature and simulation studies of competitive adsorption. Therefore, the need for research on competitive adsorption is substantial and expanding.

This review paper covers the modeling and simulation of multi-component adsorption systems. An extensive list of multi-component isotherm models is compiled. The most common single-component adsorption models are the Henry model, Langmuir isotherm model, Brunauer–Emmett–Teller (Lee and Stenstrom 1996), Freundlich isotherm model, Langmuir Freundlich hybrid isotherm model (Al-Duri 1995), Modified Competitive Langmuir (Sohn and Kim 2005), Langmuir Extension First Approximation model (Lee and Stenstrom 1996), Freundlich-Langmuir-Jovanovic (Field 2017), Modified Langmuir Freundlich model (Jeppu and Clement 2012), and LeVan–Vermeulen model (Jadhav and Srivastava 2019) which are stated with their significance and equations. Currently, 26 multi-component and 10 single-component isotherm models are discussed. Also, four multi-component isotherm models were used to simulate three binary adsorption systems.

2 Adsorption Isotherms Models

The adsorption behavior relies on solute-to-adsorbent molecular interactions in an adsorption system (Bonilla-Petriciolet et al. 2017). At a specific temperature, the equilibrium adsorbate concentrations in the aqueous phase and the solid phase are said to be isothermal. Isotherm equations are utilized to simulate the equilibrium adsorption data and examine adsorption information, adsorption mechanisms, and the maximum adsorption capacity of a system (Wang and Guo 2020). Isotherm equations provide a mathematical relationship between the adsorbate concentrations in the liquid phase and the adsorbent in the solid phase. The isotherm model seeks to establish the maximum adsorption capacity and suitability of particular adsorbates for the specific adsorbent. There are two phases of interaction, the first is solvent and solution, and the second is solid. It relies on the adsorption system's equilibrium concentrations and various component concentrations (Beyan et al. 2022). The

complexity of all the components in the adsorption system needs to be analyzed. The equilibrium isotherms plot the component equilibrium concentrations and adsorption measured at various experimental conditions (Manning and Goldberg 1996). Adsorption isotherm models correlate adsorbate and adsorbent performance at certain experimental conditions, including pH, temperature, the concentration range of interest for adsorbent and adsorbates, and pressure. It also gives the flow rate in the case of column bed adsorption.

The isotherm models are classified as single and multi-component adsorption (Bonilla-Petriciolet et al. 2017). Both single-component and multi-component adsorption systems with substantial isotherm models are provided. It is proposed that isotherm models and their coefficients can be used to build adsorption systems (Al-Ghouti et al. 2010). It may contain linearized and non-linearized forms of equations. The equilibrium parameters, heterogeneity factor, interaction coefficient, model constants, distribution coefficient, and affinity parameter are all estimated. Non-interaction between adsorbents and adsorbates, antagonistic and synergetic behavior, optimum adsorption capacity, and selection of adsorbent for particular adsorbate are assessed (Baig et al. 2009; Weerasundara et al. 2021; Wu et al. 2007).

There are some criteria for selecting the optimum isotherm model. The isotherm function and the experimental data must correlate effectively is the first criterion for choosing the best isotherm model. Second, the isotherm's function ought to be thermodynamically rational. It must satisfy three requirements: first, the isotherm must be linear when the concentration approaches zero; second, there must be a finite capacity at the maximum concentration; and third, the slope must be positive at all concentrations (Al-Ghouti and Da'ana 2020). Usability is the third factor to consider when selecting the optimal isotherm model. Ideally, the isotherm should apply to all computations, such as converting concentration to find capacity and vice versa for only some cases.

Fitting of isotherm models to experimental data is traditionally done by linear regression. Consequently, linear regression has been recognized as one of the most practical methods for establishing the best-fitting relationship, quantifying the distribution of adsorbed materials, validating the accuracy of isotherm model predictions, and quantitatively analyzing the adsorption system. However, using parameter estimation tools and least square minimization of errors is a better approach (Jeppu and Clement 2012). The fit of isotherm models to experimental data is enhanced for a given concentration range by increasing the number of isotherm parameters and minimizing the error function (Chen et al. 2022b). The error is more if the experimental data and the data from the isotherm model are distinct; the error will be minor if they are close. The optimal model can be determined by calculating several mathematical error functions.

The literature cites many works and research on the simultaneous removal of pollutants. This work highlights the various conditions and factors that contribute to adsorption. Adsorbent type, adsorbate count, temperature, adsorbate and adsorbent concentration, agitation, pH, contact duration, adsorption capacity, and surface area are the components. Furthermore, this study also provides several examples of the simultaneous removal of contaminants from literature. The lower the initial concentration of the component, the better the adsorbent sorption affinity to the adsorbate molecule is (Girish 2018). The adsorbents' activity and regeneration are influenced by temperature. While activated carbon typically requires a lower temperature, zeolites demand a high temperature (Yang 2003). The higher the surface area of the adsorbent, the more the adsorption. The pH influences the metal solubility and the dissociation degree of functional groups on the surface of sorbents. Due to the electrostatic attraction between metal ions and protonated ones, the adsorption capacity rises with increasing pH but can also fall at a specific maximum pH (Qiao et al. 2014). As adsorbent dosage boosts, the surface area increases and the adsorption rate improves,

Table 1 Influencing factors of adsorption equilibrium

No.	Factors	Significance	References
1	pH	pH is the critical parameter for adsorption. The adsorption percentage changes with changing pH values. An essential factor in assessing the quality of wastewater is the pH level. Surface charge and surface hydrolysis are impacted. In an aquatic environment, pH fluctuations regulate biological activity and chemical processes. When pH falls below zeta potential values, the surface of adsorbents will be positively charged due to protonation. Adsorbents that are positively charged will electrostatically attract negatively charged contaminants and vice versa. In an acidic solution, anionic pollutants adsorb more, and in an alkaline solution, cationic contaminants adsorb more	Ahechti et al. 2022; Chen et al. 2022b; Jeppu and Clement 2012
2	Adsorbent dosage	Dosage directly influences the adsorption capacity of a system. Efficiency is directly proportional to the adsorbent dosage as active sites increases. The adsorption rate decreases as the binding sites diminish; hence, competition between the metal ions is for fewer active sites	Ezeonuegbu et al. 2021; Girish 2019; Ramesh et al. 2012
3	Agitation speed	The agitation speed influences the quality of the reactant's dispersion and mass transfer. It ensures the uniform suspension of adsorbents and adsorbates in a solution. It has frequently been noted that, as agitation speed rises, so does the elimination percentage. Agitation causes the effective diffusion of the ions toward the adsorbents. Slower agitation might cause adsorbent particles to build up in a sample solution	Acosta-Herrera et al. 2021; Darweesh et al. 2022; Tien 2019
4	Contact time	With a shorter contact period, the adsorption process is more cost-effective. Because the boundary layer becomes a barrier to mass transfer around the sorbent molecules and it is lowered with the increased contact time, then the removal efficiency improves. The appropriate contact time is established once the ideal pH and concentration can be established. A reasonable time for adsorption is sought after contact time determination. If the contact time is too long, the adsorbent may begin to desorb	Ezeonuegbu et al. 2021; Istratie et al. 2019; Kurniawati et al. 2021

Table 1 (continued)

| No.	Factors	Significance	References
5	Coexisting ions	The complexity of a system rises as the number of pollutants does. Pollutants can coexist with anionic or cationic ions. Other ions might make the adsorption intake and removal less effective. It is because there are a certain number of binding sites for surface adsorption	Chen et al. 2022a; Noroozi and Sorial 2013; Weerasundara et al. 2021
6	Surface area	It increases the number of adsorption-active sites. Smaller particles have a greater specific surface area and more reactive atoms per unit volume, substantially accelerating the dissolving process. Micropores could be the primary element affecting sorption capacity since they comprise the most significant portion of the specific surface area. The surface area alters if chemicals are placed in a vacuum or frozen	Abbas et al. 2020; Babatunde et al. 2022; Kondor et al. 2021; Malvar et al. 2020
7	Temperature	The ideal temperature determines the adsorbents' activation and regeneration. The electrostatic connections between the metal ions weaken at high temperatures. Temperature controls the solubility of gases and salts and is crucial in evaluating wastewater quality. The temperature also impacts adsorption behaviour, changing temperature and momentum, causing components to feel kinetic energy. Higher temperatures may desorb the contaminants that have been adsorbed and reduce surface activity. As a result, the adsorption rate reduces at higher temperatures	Babatunde et al. 2022; Ezeonuegbu et al. 2021; Yang 2003
8	Concentration of adsorbate	As adsorbate concentrations rise, inter-adsorbate interaction also rises. Adsorption slows as contact time increases until saturation because fewer adsorption sites are accessible to the remaining metal ions in the solution, causing repulsive interactions between solute molecules. A significant number of accessible adsorption sites compared to the initial concentration of the adsorbate ions may be the source of the initial quick adsorption. As a result, less percentage of ions are removed. At this stage, the uptake rate is controlled by the ion transfer rate from the exterior to the interior locations of the adsorbent particles	Arim et al. 2018; Roy and Bhattacharya 2013; Darweesh et al. 2022
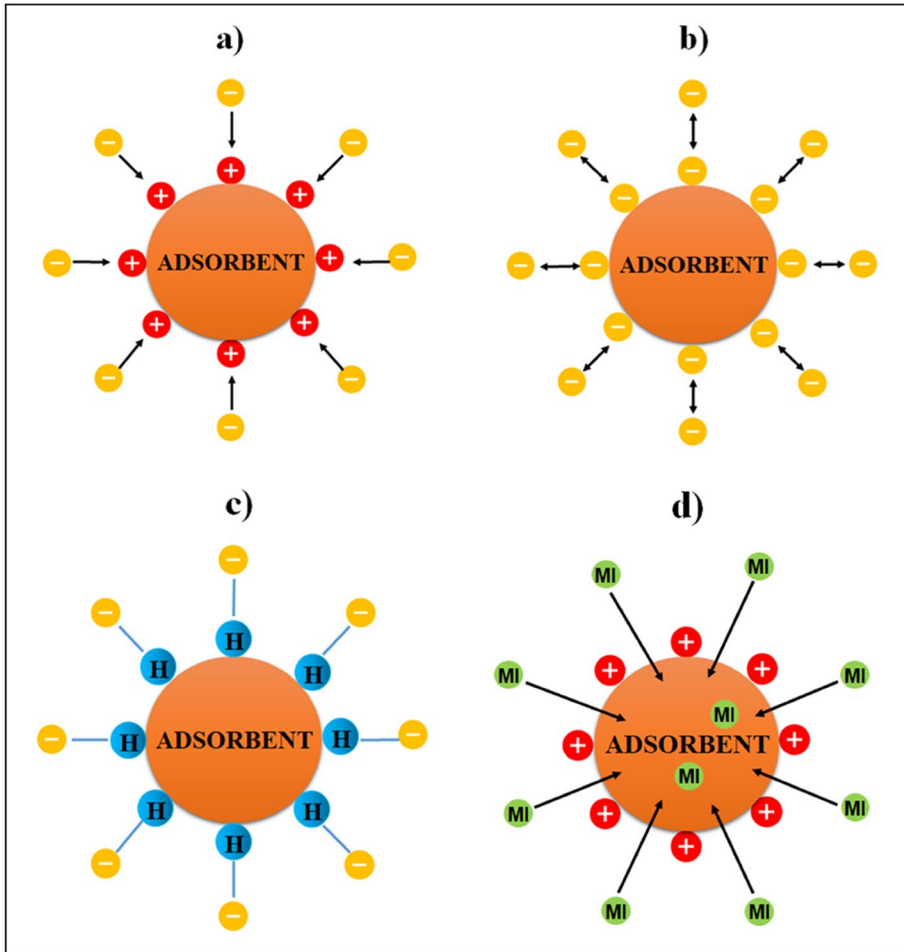
Fig. 4 Schematic diagram of (**a**) Electrostatic attraction, (**b**) Electrostatic repulsion, (**c**) Hydrogen bond, and (**d**) Metal ion exchange between adsorbents and adsorbates

providing more sites for heavy metal adsorption (Sun et al. 2019). Table 1 summarises the influencing factors of adsorption equilibrium.

2.1 Single Component Adsorption Isotherm Models

Single-component adsorption isotherm models are mathematical models used to describe the relationship between the concentration of a solute in a solution and the amount of solute adsorbed onto a solid surface. The isotherm models are called "single components" because they consider the adsorption of only one solute at a time without assuming any interactions with other solutes. The adsorption of a single component on a uniform solid surface exhibits single adsorption energy and uniform adsorption sites (Babatunde et al. 2022). Understanding single-component equilibrium studies and the basic principles of

retention processes of specific pollutant concentrations present in an adsorption system are essential (Piplai et al. 2018). The formation of electrostatic attraction and repulsion, hydrogen bond, and metal ion exchange between adsorbents and adsorbates at favorable conditions are shown in Fig. 4 (Cobbina et al. 2019). For the selection of isotherm models, theoretical and experimental guidance from the literature is available. Table 1 presents single-component removal models for one, two, and three parameters. Surface heterogeneity and homogeneity are basic assumptions in single-component models. In addition, it is also assumed that adsorption may be monolayer or multilayer (Van Assche et al. 2018). Single-component models are the foundation for many multi-component models. Table 1 represents the principal equilibrium isotherm models for single components and the prior significance, equations, and experimental factors influencing the equilibrium adsorption phenomena.

2.2 Multi-Component Adsorption Isotherm Models

In the study of adsorption, multi-component adsorption is of crucial relevance. In addition to the solid–liquid adsorption phase, competition phenomena might occur in a solid–solid adsorption stage. When there is more than one contaminant, additional experimental work is necessary. Because there are more contaminants in the adsorption system, multi-component equilibria are more complicated (Bonilla-Petriciolet et al. 2017). The interaction of the various pollutants makes it impossible to measure them experimentally using current techniques since they depend on the concentration of the other component in the same adsorption system (Yang 2003). In a multi-component system, it is exceedingly difficult to predict the individual and competitive interaction during migration, the separation process, and the optimal experimental circumstances (Girish 2018). Despite this, several factories and industries release many pollutants simultaneously, such as organic and inorganic salts, heavy metals, proteins, and various behavioral characteristics. Therefore, they must simultaneously be removed from the polluted water (Girish and Murty 2016).

Competitive adsorption is influenced by the physical characteristics of the adsorbents, including surface charge density, surface area, particle size, and porosity (Bansal and Goyal 2005). Additionally, factors like adsorbent size, agitation rate, pollutant characteristics or ions that need to be removed, contaminant concentration, ion to ion interactions, affinity of an ion species for the adsorbent, and interest in the active sites of adsorbents are also considered (Bibi et al. 2015). Multi-component adsorption equilibria define the quantitative link between the adsorbates and adsorbents in the solution and the number of solutes adsorbed by the adsorbent (González-López et al. 2022). As shown in Table 2, many multi-component isotherms have a variety of assumptions and relevance.

The most vital scenario of competitive adsorption model determinations depends on the parameters of the corresponding single-component isotherms. Comparatively single isotherm models are uncomplicated, accurate and precise. A schematic representation of multi-component adsorption is given in Fig. 5. Multi-component isotherm models are effectively used for the combination of pollutants. Some are the Extended Langmuir isotherm, Modified Competitive Langmuir isotherm, and Langmuir Extension First Approximation Equilibrium isotherm models. Twenty-six multi-component isotherms are presented in Tables 2 and 3, along with the nonlinear equations and their significance.

Table 2 Single-component parameter-based nonlinear equations

No.	Isotherm model	Qe (non-linear)	Parameters	Significance	Ref.
1	Mono-parameter Henry Isotherm Model (HI)	$Q_e = K_{H_e} C_e$	K_{H_e}	It has only a linear form of the equation. It is the most straightforward method for the study of adsorption isotherm	Formstedt 2010
2	Two-parameter Langmuir Isotherm Model (LI)	$Q_e = Q_m \dfrac{k_L C_e}{1+k_L C_e}$	k_L, Q_m	It assumes the formation of a monolayer, homogenous surface, and no interactions between the adsorbates. The adsorbent sites will have the same energy to attract the adsorbates	Li et al. 2003
3	Freundlich Isotherm Model (FI)	$Q_e = K_F C_e^{1/n}$	K_F, n	A reversible multilayer on the heterogeneous surface is established. The distribution of components depends on the time and energy of the sites ensured	Febrianto et al. 2009
4	Langmuir Freundlich Hybrid Isotherm Model (LFHI)	$Q_e = \theta = \dfrac{q_e}{q_a} = \dfrac{\left[K_L\left(\frac{c_S}{c_0}\right)\right]^m}{1+\left[K_L\left(\frac{c_S}{c_0}\right)\right]^m}$	K_L, m, C_S	This isotherm is the application of Langmuir isotherm on a heterogeneous surface. Quasi-Gaussian distribution is implied	Al-Duri 1995
5	Brunauer, Emmett, Teller (BET Isotherm)	$Q_e = \dfrac{BCQ_m}{(C_s-C_e)\left[1+(B-1)\left(c_e/c_S\right)\right]}$	B, C_s, C	It almost follows the Langmuir isotherm assumptions but is a multilayered adsorption system. It implements a Langmuir isotherm in each adsorption layer	Lee and Stenstrom 1996
6	Three-parameter Toth Isotherm Model (T model)	$Q_e = \dfrac{K_T C_e}{(a_T+C_e)^{\frac{1}{t}}}$	K_T, a_T, t	It has the vital function of operating both in low and high concentrations. Langmuir model is modified to diminish the errors between experimental and predicted data	Al-Ghouti and Da'ana 2020
7	Sips Isotherm Model (SP)	$q_e = \dfrac{K_s C_e^{\beta_s}}{1+K_s C_e^{\beta_s}}$	K_s, β_s	There is a subtle blend of Langmuir and Freundlich models and limits to follow the Henry model at low concentrations. This model is essential to identify the heterogeneity of the surface at high concentrations	Al-Ghouti and Da'ana 2020
8	Redlich Peterson Isotherm Model (RPI)	$Q_e = \dfrac{k_{RP} C_e}{1+a_{RP} C_e^{\beta}}$	$k_{RP}, \alpha_{RP}, \beta$	It obeys Langmuir and Freundlich models, but it is not monolayer adsorption. It will pertain to either homogeneous or heterogeneous surfaces	Girish 2019

Table 2 (continued)

No.	Isotherm model	Qe (non-linear)	Parameters	Significance	Ref.
9	Modified Langmuir Freundlich Isotherm Model (MLF)	$Q_e = Q_m \frac{[C_e k_a]^n}{1+[C_e k_a]^n}$	k_a n, Q_m	The uniqueness of this isotherm is its pH dependency. The essential experimental condition required to apply this isotherm model in a system is pH	Jeppu and Clement 2012
10	Khan Isotherm Model (KI)	$Q_e = \frac{q_s b_k C_e}{(1+b_k C_e)^{a_k}}$	b_k, a_k, q_s	It applies only to sterile solutions. Depending on the exponential model component, it behaves as Langmuir and Freundlich isotherm models	Khan and Ataullah 1997

Table 3 Multi-component adsorption isotherms models with nonlinear equations and their significance

No.	Isotherm model	Isotherm equations	Parameters	Significance	References
1	Extended Langmuir Isotherm/Non-modified Langmuir Isotherm Model (EL)	$Q_{e,i} = Q_{m,i} \dfrac{K_{L,i} C_{e,i}}{1 + \sum_{j=1}^{N} K_{L,i} C_{e,i}}$	$K_L, Q_{m,i}$	In this model, interaction amongst the adsorbates after adsorption is not considered: furthermore, it assumes a homogenous surface and equal distribution of adsorbed sites to the adsorbents	Srivastava et al. 2008
2	Extended Langmuir–Freundlich Isotherm Model (LF)	$Q_{e,i} = Q_{m,i} \dfrac{K_{LF,i} C_{e,i}^{\left(1/n_i\right)}}{\sum_{j=1}^{N} K_{LF,i} C_{e,i}^{\left(1/n_i\right)}}$	$K_{LF}, n, Q_{m,i}$	Prediction of adsorption data by the Langmuir isotherm has some limitations. Hence the Freundlich expression is added to the Langmuir isotherm to minimize the limits	Costa et al. 2019
3	Modified Competitive Langmuir Isotherm Model (MCL)	$Q_{e,i} = Q_{m,i} \dfrac{K_{L,i} (C_{e,i}/n_{L,i})}{1 + \sum_{j=1}^{N} K_{L,i} (C_{i,j}/n_{L,j})}$	$K_L, n_L, Q_{m,i}$	This isotherm can also explore the interaction term and affinity towards the sites by each component. Depending on the interaction coefficient, adsorption behavior like antagonistic/synergistic is known	Sohn and Kim 2005
4	Langmuir Extension First Approximation Model (LEFA)	$Q_{e,i} = \dfrac{A_i C_{e,i} + A_{ij} C_{e,i} C_{e,j}}{1 + B_i C_{e,i} + B_j C_{e,j} + B_{ij} C_{e,i} C_{e,j}}$ $Q_{e,j} = \dfrac{A_j C_{e,j} + A_{ji} C_{e,i} C_{e,j}}{1 + B_i C_{e,i} + B_j C_{e,j} + B_{ij} C_{e,i} C_{e,j}}$	A, B	The assumption of this isotherm is that the adsorption and desorption rates are linear functions. Initially, the desorption rate was neglected	Lee and Stenstrom 1996
5	Extended Freundlich Isotherm Model (EF)	$Q_{e,i} = \dfrac{K_{F,i} C_{e,i}^{\left(1/n_i\right)+x_i}}{C_{e,i}^{x_i} + y_i C_{e,j}^{z_i}}$ $Q_{e,j} = \dfrac{K_{F,j} C_{e,j}^{\left(1/n_j\right)+x_j}}{C_{e,j}^{x_j} + y_j C_{e,j}^{z_j}}$	K_F, x, y, z, n	The Freundlich isotherm for monocomponent gave the best results, modified with exponential distribution. Even though it is competitive adsorption, each monocomponent system can be fetched	Padilla-Ortega et al. 2013

Table 3 (continued)

No.	Isotherm model	Isotherm equations	Parameters	Significance	References
6	Non-Modified Competitive Redlich Peterson Isotherm Model (NMCRP)	$Q_{e,i} = \dfrac{K_{RP,i}C_{e,i}}{1+\sum_{j=1}^{N}\left\{\alpha_{RP,j}C_{e,j}^{\beta j}\right\}}$	$K_{RP}, \alpha_{RP}, \beta$	It is a combination of Langmuir and Freundlich. It acquires to be different isotherms at a wide variety of concentration changes. It behaves as FI when concentration is high and $\beta = 0$. It acts as LI when concentration is low and $\beta = 1$	Girish 2019
7	Modified Competitive Redlich Peterson Isotherm Model (MCRP)	$Q_{e,i} = \dfrac{K_{RP,i}(C_{e,i}/\eta_{RP,i})}{1+\sum_{j=1}^{N}\left\{\alpha_{RP,j}\left(\frac{C_{e,j}}{\eta_{RP,j}}\right)^{\beta j}\right\}}$	$K_{RP}, \alpha_{RP}, \beta, \eta_{RP}$	MCRP is amended with the interaction factor, suggesting the competition between the adsorbents and adsorbates. Antagonistic, synergistic, or no interaction behavior of adsorption can also be studied	Al-Ghouti and Da'ana 2020
8	Sheindorf–Rebuhn–Sheintuch (SRS) Isotherm Model	$Q_{e,i} = K_{F,i}C_{e,i}\left\{\sum_{j=1}^{N}\left(a_{ij}C_{e,i}\right)\right\}^{(1/n_i)-1}$	K_F, a, n	The competition co-efficient is an additive assumption to FI, defining adsorption energy distribution between the molecules. The interaction factor gives the relationship between the components present in the solution	Girish 2019
9	Extended Sips Isotherm Model (ES)	$Q_{e,i} = \dfrac{Q_{m,i}K_{s,i}C_{e,i}^{m}}{1+\sum_{j=1}^{N}K_{s,i}C_{e,i}^{m}}$	$K_s, Q_{m,i}, m$	This multi-component adsorption is for heterogeneous systems, at high concentration $m=1$ and low concentration $m=0$ for the contaminants	Al-Asheh et al. 2000

Table 3 (continued)

No.	Isotherm model	Isotherm equations	Parameters	Significance	References
10	Jain- Snoeyink Isotherm Model (JS)	$Q_e = \dfrac{(Q_{maxi} - Q_{maxj})K_i C_i}{1+K_i C_i} + \dfrac{Q_{maxj} K_i C_i}{1+K_i C_i + K_j C_j}$ Where $\left(Q_{maxi} > Q_{maxj}\right)$	K, Q_{max}	Though it is like an EL isotherm model, the additive factor is interaction, and competition between the adsorbates is considered. Each term gives adsorbate data	Guibal and Beppu 2007
11	Modified Jain- Snoeyink Isotherm Model (MJS)	$Q_{e,i} = \dfrac{\left(Q_{maxi}^0 - Q_{maxj}^0\right)K_{Li}^0 C_{ei}}{1+K_{Li}^0 C_{ei}} + \dfrac{Q_{maxj}^0 K_{Li}^0 C_{ei}}{1+K_{Li}^0 C_{ei}+K_{Lj}^0 C_{ej}}$ $Q_{e,j} = \dfrac{Q_{maxj} K_{Lj} C_{ej}}{1+K_{Li} C_{ei}+K_{Lj} C_{ej}}$ Where $\left(Q_{maxi}^0 > Q_{maxj}^0\right)$	K_L, Q_{max}	It is an improved version of the JS model, wherein the equation introduces the interaction term. On this condition, one of the maximum adsorption capacities of a component must be greater than that of the other	Yazdani et al. 2012
12	Steric Mass Action (SMA) Isotherm Model	$Q_i = \dfrac{K_i \left(Q_0 - \sum_{j=1}^{N} (z_j + \sigma_{S,j}) Q_i\right)^{z_i}}{(c_{cl^-})^{z_i}} c_{e,i}$	$K, Q_0, z, \sigma_S, c_{cl^-}, Q_j$	Protein adsorption is the aim of this isotherm. A counter ion parameter of salt was initiated for single-component adsorption. Then further same was applied for multi-component adsorption theoretically, which was unsuccessful	Field 2017
13	Freundlich- Langmuir- Jovanovic Isotherm Model (FLJ)	$Q_i = \dfrac{\Lambda K_i C_{eqi}^{a_i} exp(-A_i \cdot C_{Cl^{-1}})}{1+\sum_{j=1}^{N} K_j C_{eqj}^{a_j} \cdot exp(-A_j \cdot C_{Cl^{-1}})}$	$\Lambda, \alpha, A, C_{Cl^{-1}}$	It is like the SMA model for adsorbing protein. An extra exponential salt parameter was considered for the multi-component adsorption	Field 2017

Table 3 (continued)

No.	Isotherm model	Isotherm equations	Parameters	Significance	References
14	LeVan–Vermeulen Isotherm Model (LV)	$Q_1 = \dfrac{Q_m^* K C_{e,i}}{1+\sum_{j=1}^N K_j C_{e,j}}$ $+c_{e,i}\left\{\dfrac{\sum_{j=1}^N K_i K_j C_{e,j}(Q_{m,i}-Q_{m,i})}{\left(\sum_{z=1}^n K_j C_{e,j}\right)^2}\right\}\ln\left(1+\sum_{j=1}^N K_j C_{e,j}\right)$ Where $Q_m^* = \sum_{i=1}^N \left(\dfrac{Q_{m,i} K_i C_{e,i}}{K_i C_{e,i}}\right)$	Q_m^*, K	It can be valid only if it follows Langmuir isotherm and competitive adsorption between pure components. It is improvised using the IAST model, as there was an inconsistency in the Modified Langmuir isotherm model	Jadhav and Srivastava 2019
15	Empirical Bisolute Extension of the Freundlich Isotherm Model (EBEF)	$Y_i = \dfrac{a_i X_i^{b_i+b_{ii}}}{X_i^{b_{ii}}+a_{ij}X_j^{b_{ij}}}\left(\lim_{c_i\to 0} Y_i = a_i X_i^{b_i}\right)$ $Y_j = \dfrac{a_j X_j^{b_j+b_{jj}}}{X_j^{b_{jj}}+a_{ji}X_i^{b_{ji}}}\left(\lim_{c_j\to 0} Y_j = a_j X_j^{b_j}\right)$ Where $Y_i = a_i X_i^{b_i}$ or $Q_e = KC^n$	$X, Y, a, b, a_{ij}, a_{ji}, b_{ij}, b_{ji}, b_{ii}, b_{jj}$	It is a rarely used isotherm model because of its complexity with six parameters. Some of the interaction parameters must be derived from the experimental values	McKay and Al-Duri 1991
16	Ideal Adsorbed Solution Theory Freundlich Isotherm Model (IASFC) / Crittenden et al.'s IAS-Freundlich Isotherm model	$C_i = \dfrac{q_i}{\sum_{j=1}^N q_j}\left(\dfrac{\sum_{j=1}^N n_j q_j}{n_i K_i}\right)^{n_i}$ Based on $Q_e = KC^{1/n}$ For Binary systems, $c_i = \dfrac{q_i}{q_1+q_i}\left(\dfrac{n_1 q_1 + n_i q_i}{n_i K_i}\right)^{n_i}$ $c_2 = \dfrac{q_i}{q_i+q_i}\left(\dfrac{n_1 q_1 + n_i q_i}{n_i K_i}\right)^{n_i}$	K, n	The uniqueness of this isotherm is that it is successful for competitive adsorption of binary, ternary, till six solute systems. The applied solute systems must follow a single pollutant system. Freundlich isotherm linear log–log plots. If there is an error in computation, this isotherm cannot be implied for competitive adsorption	Crittenden et al. 1985

Table 3 (continued)

No.	Isotherm model	Isotherm equations	Parameters	Significance	References
17	Ideal Adsorbed Solution Theory Freundlich Isotherm Model (IASFF) / Fritz and Schlunder's IAS-Freundlich Model	$\frac{y_i^0}{b_{ik}} - C_{i,k} = \frac{y_j^0}{b_{j,k}} - C_{j,k}$ $X_i = X_i^0 Z_i$ $X_j = X_j^0(1 - z_i)$ $\frac{Y_i}{y_i^0} + \frac{Y_j}{y_j^0} = 1$ Where $Y_i = a_i X_i^{b_{ik}}$ or $Q_e = KC^n$ or $Q_{e,i} = K_{ik} C_i^{n_{ik}}$	$K, n, Y, X, a, b_k, Z, y_i^0, X_i^0, K_k$	It is a tedious method to apply as it is an integral derivation of the IAS model. Spreading IAS pressure theory employs solid–solution and solid–solvent interfaces. It mainly includes Freundlich isotherm model parameters. Further studies showed that this method is not recommended since it is complex	Fritz et al. 1981
18	Simplified Ideal Adsorbed Solution Isotherm Model (SIAS)	$Q_i = K^{\left(\frac{n'-1}{n}\right)}\left[K_i C_i^n\right]^{\frac{1}{n}}\left\{\sum_N \left(\frac{K_i}{K} C_i^n\right)^{\frac{1}{n}}\right\}^{(n'-1)}$ Where $Q_e = KC^n$	K', K, n, n'	It is familiarly used for phenolic compounds. These isotherm results are identical to the IAS isotherm model only when 'n' values are the same. But when significant changes in 'K' and 'n' values are substantial, the results are not the same	Digiano et al. 1978
19	Improved Simplified Ideal Adsorbed Solution Isotherm Model (ISIAS)	$Q_i = K^{\left(\frac{1-n'}{n}\right)}\left[\frac{K_i}{n_i} C_i^{n_i}\right]^{\frac{1}{n}}\left\{\sum_N \left(\frac{\frac{K_i}{n_i}}{K'} C_i^{n_i}\right)^{\frac{1}{n}}\right\}^{(n'-1)}$ Where $K' = \frac{\Sigma(K_i/n_i)}{N}$	K, n, n', η	It is similar to the SIAS model except for interaction co-efficient (η), which is related to the solubility factor. It gave the best results under non-ideal conditions than the LI, IAS, and SIAS models, as the error residual of the sum of squares incurred was minimal	Lee and Stenstrom 1996

Table 3 (continued)

No.	Isotherm model	Isotherm equations	Parameters	Significance	References
20	Ideal Adsorbed Solution (IAS) Isotherm Model	a) $\pi_i = \frac{RT}{A} \int_0^{C_i^0} \frac{Q_{e,i}^0(C_i^0)}{C_i^0} \cdot dC_i^0$ b) $\pi_i = f_i(C_i^0)\,\pi_j = f_j(C_j^0)$ c) $C_i = C_T X_i = C_i^0 Z_i C_T X_j = C_j^0(1 - Z_j)$ d) $\sum_{i=1}^N z_i = z_i + z_j = 1$ e) $Q_{e,i} = Q_{e,T} * z_i$ f) $\frac{1}{Q_{e,T}} = \sum_{i=1}^N \frac{z_i}{Q_{e,i}^0} = \sum_{i=1}^2 \frac{z_i}{Q_{e,i}^0}$ g) $Q_{e,i} = \frac{(C_{i,0} - C_i)V}{M}$ h) $\pi_i = \pi_j = \pi_{mix}$	$R, T, A, z_i,$ $X_i,$ C_T	Though it is a base of many models, it possesses some limitations. Among all the discussed models above, the IAS model is very complex. It is commonly used for volatile organic compounds, dilute solutions, and similar surface areas for adsorbents taken at the same temperature and spreading pressure. It can be applied only to binary systems. If the 'n' value increases for more competitive adsorption studies, at the same time, the number of equations also increases as it consists of separate single solute equations	Radke and Prausnitz 1972
21	Polanyi's Potential Theory Isotherm Model (PPT)	$A = RT ln\left[\frac{P_s}{P}\right]$	R, T, P_s, P	This model applies adsorption potential to gas and vapor adsorption by considering the distance between adsorbate and adsorbent. It is temperature-independent adsorption, which depends on the pressure until it reaches saturation. Later these phenomena are implemented on aqueous solution adsorption	Stoeckli 1998
22	Solubility normalized Isotherm Model (S model)	$A = RTln\left[\frac{C_S}{C}\right]$ Where $C_s = 100 \times exp\left[\frac{v_A}{v_T} - 1 - \frac{v_A}{RT}(\delta_A - \delta_T)^2\right]$	$R, T, C_S, v_A,$ v_T, δ_A, δ_T	They are extensively used for the treatment of wastewater for organic compounds	Giraldo et al. 2013

Table 3 (continued)

No.	Isotherm model	Isotherm equations	Parameters	Significance	References
23	Non-normalized Isotherm Model (C model)	$A = RT ln\left(1 + \frac{1}{C_e}\right)$	R, T	Polycyclic molecules such as dyes are adsorbed, and the adsorption potential is examined. It does not have any theoretical explanation but helps compute metal ions	Giraldo et al. 2013
24	Modified Polanyi Potential Isotherm Model (MPP)	$A = RT ln\left(1 + \frac{C^0}{C_e}\right)$	R, T, C^0	The computations are different, like the Dubinin Radushkevitch isotherm model	Zhou 2020
25	Dubinin Astakhov Isotherm Model (DA Model)	$N_{ads} = N_{ads,max} exp\left[-\left(\frac{A}{E}\right)^n\right]$	A, E, n	This model is derived from S or C model by considering distribution parameters and temperature-independent factors. It is mainly employed for the adsorption of dyes from an aqueous solution	Stoeckli 1998
26	Dubinin Radushkevitch Isotherm Model (DR Model)	$ln Q_e = ln q_{max} - \beta \varepsilon^2$ Where $\varepsilon = RT ln\left(1 + \frac{1}{C_e}\right)$	$\beta, \varepsilon, q_{max}$	It depends on the solid-aqueous phase adsorption and is entirely temperature-independent. It counts the free energy concept in adsorption	Zhou 2020

3 Competitive Removal of Pollutants

The removal of multiple pollutants in a multi-component adsorption system is crucial. Multi-component adsorption is significant because the waste streams and groundwater contain a mixture of contaminants such as arsenic and fluoride, cadmium and nickel, and chromium and vanadium, and removing these pollutants requires effective adsorbents. Some case studies on the simultaneous removal of commonly co-occuring heavy metals are presented in Table 4.

In case (i) Dhanasekaran and Sahu (2021) studied arsenic and fluoride adsorption on activated alumina-impregnated sawdust. The adsorption capacity of 0.10 mg/g of arsenic and 2.42 mg/g of fluoride was obtained in the binary system at pH 6–7. The Freundlich isotherm model was used to predict and simulate the equilibrium data. In case (ii) bagasse active carbon was successfully employed to extract zinc and cadmium at pH 4.5. The adsorption followed both Langmuir and Freundlich isotherm models. Comparatively, the Freundlich model provided a better fit (Mohan and Singh 2002). Further, Padilla-Ortega et al. (2013) demonstrated that vermiculite has stronger selectivity of Pb(II) in single-component adsorption than copper in case (iii). Even in competitive adsorption, Pb(II) has more affinity towards vermiculite (0.579 mg/g) than Cu(II) (0.513 mg/g). But both metals can be desorbed with presence of other metals in the adsorption system. Vermiculite removed about 88% of lead and 58% of copper at pH 4.

Similarly, Padilla-Ortega et al. (2013) also investigated the simultaneous removal of Cd and Ni onto bentonite in case (iv). Their research findings indicated that Cd(II) has a better affinity to bentonite than Ni(II) in a single-component system. In the competitive adsorption system, both metals displayed antagonistic behavior against the presence of other metals. Both metals have a relatively comparable affinity for bentonite. In case (v) Padilla-Ortega et al. (2013) gave the equilibrium adsorption studies of cadmium and zinc onto sepiolite in a single-component system at pH 7. It was demonstrated that cadmium was adsorbed 1.3 times more than zinc. However, in a competitive adsorption system, the behavior was different. Zn(II) presented assertive antagonistic behavior over Cd(II) adsorption. Cd(II) did not affect the adsorption of Zn(II). Nevertheless, in case (v), the presence of Zn(II) reduced the uptake of Cd(II) up to 16.5 times due to the same cationic sites on the adsorbent.

Roy and Bhattacharya (2013) used maghemite nanotubes to remove Cd(II) and Ni(II) from wastewater of chemical, metallurgical, and textile industries as in case (vi). Binary adsorption investigations showed Cd(II) affinity (88.14 mg/g) was better than that of Ni(II) (70.12 mg/g). The adsorption of a single ion system got better when the pH increased. Cd(II) gets strongly influenced by Ni(II). Correspondingly, Nickel and cobalt adsorption on γ-Fe_2O_3 nanotubes was also investigated in case (vii) by Roy and Bhattacharya (2013). Ni(II) absorbs way more than Co(II) in a single adsorbent system. The adsorption efficiency from a single to a binary system has almost no change for cobalt. The adsorption capacity for Ni(II) was 65.62 mg/g and for Co(II) 58.83 mg/g in a binary system. In this study, the higher the pH value of a single ion, the better the adsorption. The potential of maghemite nanotubes was also verified for cadmium and copper by Roy and Bhattacharya (2013). Cadmium adsorption was successfully higher than that of cobalt in a single-component system. The adsorption capacity for Cd(II) was 55.87 mg/g and for Co(II) 85.27 mg/g in a binary system. Cd(II) adsorption decreased firmly in the presence of Co(II) in case (viii). The adsorption of a single ion system got better when the pH increased. Table 4 summarizes the above case studies with different experimental conditions, isotherm models, and significance.
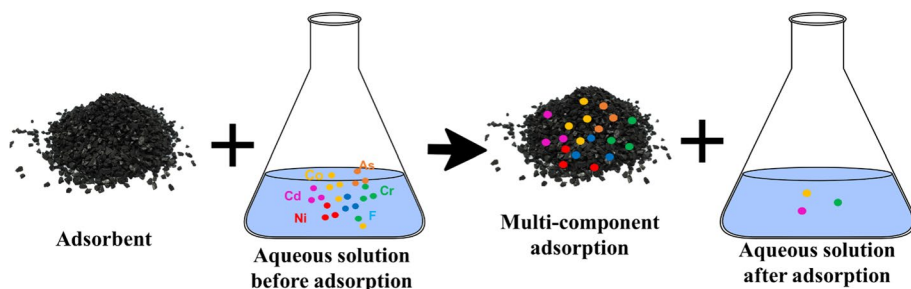
Fig. 5 Schematic representation of multi-component adsorption

4 Interaction Mechanism of Competitive Adsorption

The mechanisms of pollutants are the most significant phenomena in multi-component adsorption equilibria. Gaining a deeper understanding of these mechanisms is essential in achieving better results and analyzing any adsorption system. One of the primary considerations for sorbent design is the van der Waals interactions since adsorption depends on the charge of the sorbate molecules and the atoms on the sorbent surface. The van der Waals radius and particle surface charges determine the interactions. The polarizability of the surface atom, which rises with the atomic weight of elements, enhances the dispersion interaction for a sorbate molecule (Yang 2003). Figure 6 shows the interaction between two adsorbents affecting adsorption in a binary system.

Synergism is one of the three primary methods through which adsorbate molecules interact. It describes how combining two components in a solution improves the ability of the pollutant to adsorb when compared to using only one (Bohli et al. 2017). Additionally, the process is referred to as no interaction when the presence of another pollutant does not impact how well the other contaminant is adsorbed in a binary solution. Every element of a single system is equally essential to a binary system. The last primary interaction is the opposite of synergism, called antagonistic. When a component is present in a solution with another element, its adsorption ability becomes less effective.

There is synergism when the ratio of the adsorption capacity of a component in a binary system to that in a single system is higher than one. If it is less than one, then there is antagonism. If this ratio is equal to one, then there is no interaction. This is called the additive rule. The relative percent adsorption R_Q explains the interaction mechanism used (Sağ et al. 1998). There is no molecular interaction if the value of R_Q is 100. If the value of R_Q is below 100, this indicates antagonistic interactions, whereas a value above 100 describes synergistic interactions (Girish 2018). Selectivity is a crucial component in the explanation of the adsorption mechanism. It characterizes a component's discrimination when it competes against two or more other elements in the same solution (Zhang et al. 2019).

The selectivity ratio determines the selective preference of an adsorbent for a component. This ratio decides between binary and single systems based on morphology, surface structure, and pore distribution (Girish 2018). Furthermore, the interactions of molecules are described by the P-factor, a streamlined model that uses a ratio of monolayer capacity (Qmax) for the correlation approach. The P-factor contrasts data from equilibrium with many components and is dimensionless (Choy et al. 2004). Similarly, the sorption affinity helps describe reactions. The adsorption capabilities of adsorbents in a binary system can

Table 4 Summary of simultaneous adsorption of common heavy metals in the binary system, Isotherm models, experimental conditions, and adsorption capacity of heavy metals

No.	Pollutants (adsorbate)		Adsorbents	Source of wastewater	Isotherm model used	SA (m²/g)	Experimental conditions					Co (mg/L)	
	1	2					pH	T (°C)	D (g/ml)	CT (Min)		1	2
i)	As (v)	F	Ferric hydroxide, activated alumina with sawdust (SFAA)	Groundwater	Extended Langmuir and Extended Freundlich isotherm model	22.5	6.5–7	30	0.1	5–140		0.1–2	5–50
ii)	Cd	Zn	Bagasse activated carbon	Wastewater treatment	Langmuir and Freundlich isotherm model	960	4.5	10,25,40	4–8 g/L	720		200	200
iii)	Pb	Cu	Vermiculite	Wastewater from industries, manufacturing batteries	Langmuir, Freundlich, Redlich Peterson isotherms model	15.2	4	25	0.2 g	1/40 mL Dilution Factor, 7 days		2 meq/L	1.3 meq/L
					Extended Langmuir isotherm model	15.2	4	25	0.2 g	1/40 mL Dilution Factor, 7 days		2 meq/L	1.3 meq/L
					Modified Langmuir isotherm model								
					Modified Redlich Peterson Isotherm model								
					Extended Freundlich isotherm model								
					Sheindorf Rebuhn Sheintuch isotherm model								

Table 4 (continued)

No.	Pollutants (adsorbate)		Adsorbents	Source of wastewater	Isotherm model used	SA (m²/g)	Experimental conditions				Co (mg/L)	
	1	2					pH	T (°C)	D (g/ml)	CT (Min)	1	2
iv)	Cd	Ni	Bentonite	Metal finishing industry, coolants, metal smelting Water	Langmuir, Freundlich, Redlich Peterson isotherms model	41.7	7	25	0.2 g	1/40 mL Dilution Factor, 7 days	0 – 5 meq/L	0 – 5 meq/L
					Extended Langmuir isotherm model	41.7	7	25	0.2 g	1/40 mL Dilution Factor, 7 days	0 – 5 meq/L	0 – 2 meq/L
					Modified Langmuir isotherm model							
					Modified Redlich Peterson Isotherm model							
					Extended Freundlich isotherm model							
					Sheindorf Rebuhn Sheintuch isotherm model							
v)	Zn	Cd	sepiolite	Water from mining, pesticides used in agriculture	Langmuir, Freundlich, Redlich Peterson isotherm model	194	7	25	0.2 g	1/40 mL Dilution Factor, 7 days	0 – 0.8 meq/L	
					Extended Langmuir isotherm model	194	4	25	0.2 g	1/40 mL Dilution Factor, 7 days	0.8 meq/L	

Table 4 (continued)

No.	Pollutants (adsorbate) 1	2	Adsorbents	Source of wastewater	Isotherm model used	SA (m²/g)	pH	T (°C)	D (g/ml)	CT (Min)	Co (mg/L) 1	2
					Modified Langmuir isotherm model							
					Modified Redlich Peterson Isotherm model							
					Extended Freundlich isotherm model							
					Sheindorf Rebuhn Sheintuch isotherm model							
vi)	Cd	Ni	Maghemite γ-Fe$_2$O$_3$ nanotubes	Wastewater from chemical, metallurgical, and textile industries	Langmuir, Freundlich Isotherm model	321.638	6	25	0.05 g/100 mL	240	200–400 mg/L	200–400 mg/L
vii)	Ni	Co	Maghemite γ-Fe$_2$O$_3$ nanotubes	Wastewater from chemical, metallurgical, and textile industries	Langmuir, Freundlich Isotherm model	321.638	6	25	0.05 g/100 mL	240	200–400 mg/L	200–400 mg/L
viii)	Co	Cd	Maghemite γ-Fe$_2$O$_3$ nanotubes	Wastewater from chemical, metallurgical, and textile industries	Langmuir, Freundlich Isotherm model	321.638	6	25	0.05 g/100 mL	240	200–400 mg/L	200–400 mg/L

Experimental conditions

Table 4 (continued)

No.	Isotherm Parameters K		Adsorption capacity, Qm (mg/g)				The goodness of fit (R²)		Inference and Reference
	1	2	Single		Binary		1	2	
			1	2	1	2			
i)	$K_L = 124.265$	$K_L = -0.720$	77.6	40.28	0.10	2.42	0.911	0.999	Impregnated SFAA effectively removes As and F, with pH 6–7. It follows the Freundlich isotherm model. (Dhanasekaran and Sahu 2021)
	$K_F = 211.178$	$K_F = 1.366$					0.99	0.999	
ii)	$K_L = 8.8 \times 10^{-3}$	$K_L = 8 \times 10^{-3}$	55 mol	44.8 mol	9.61	7.46	0.9678	0.9794	Bagasse can be fruitfully used to remove Cd and Zn, and the Freundlich model gave a better fit. (Mohan and Singh 2002)
	$K_F = 1.74$	$K_F = 1.42$					0.9864	0.9868	

Table 4 (continued)

No.	Isotherm Parameters K		Adsorption capacity, Qm (mg/g)				The goodness of fit (R^2)		Inference and Reference
			Single		Binary				
	1	2	1	2	1	2	1	2	
iii)	$K_L=0.984$	$K_L=0.686$	0.50 meq/L	0.46 meq/L	0.579	0.513	–	–	Pb(II) selectivity in single-component adsorption is higher on vermiculite than on Cu(II). Even in competitive adsorption, Pb (II) affinity is more than Cu(II) on vermiculite. Both metals can be desorbed with other metals in the adsorption system. Pb(II) displaces more than Cu(II), 58% and 88%, respectively. (Padilla-Ortega et al. 2013)
	$K_F=0.255$	$K_F=0.205$							
	$K_{RP}=1.52$,	$K_{RP}=0.768$,							
	$\alpha_{RP}=4.48$,	$\alpha_{RP}=2.66$,							
	$\beta=0.797$	$\beta=0.737$							
	$K_E=1.06$	$K_E=0.442$			0.545	0.545			
	$\eta=1.05$	$\eta=1.48$							

Table 4 (continued)

No.	Isotherm Parameters K		Adsorption capacity, Qm (mg/g)				The goodness of fit (R^2)		Inference and Reference
			Single		Binary				
	1	2	1	2	1	2	1	2	
	$Ƞ=0.828$ X $=0.644,$ Y $=0.137,$ Z $=1.10$ $a_{11}=1, a_{12}=0.39$	$Ƞ=1.01$ X $=0.462,$ Y $=1.32,$ Z $=0.621$ $a_{22}=1, a_{21}=5.59$							
iv)	$K_L=2.41$	$K_L=0.875$	0.64 meq/L	0.44 meq/L	0.6, 0.41,0. 33,0.3 meq/g	0,2,4,5 meq/L			Cd (II) has a better affinity than Ni(II) in a single-component system on bentonite. In the competitive adsorption system, both metals showed antagonism against the presence of other metals. The affinities towards bentonite are very similar for both metals. (Padilla-Ortega et al. 2013)

Table 4 (continued)

No.	Isotherm Parameters K		Adsorption capacity, Qm (mg/g)				The goodness of fit (R^2)		Inference and Reference
			Single		Binary				
	1	2	1	2	1	2	1	2	
	$K_F = 0.413$	$K_F = 0.246$			0,2,4, 5 meq/L	0.53, 0.39, 0.32, 0.29 meq/g			
	$K_{RP} = 1.18$, $\alpha_{RP} = 3.05$, $\beta = 0.906$	$K_{RP} = 0.753$, $\alpha_{RP} = 1.84$, $\beta = 0.829$							
	$K_E = 1.95$	$K_E = 1.86$			0.629	0.581			
	$\eta = 1.85$	$\eta = 0.569$							
	$\eta = 1.42$	$\eta = 0.614$							
	$X = 0.546$, $Y = 1.17$, $Z = 0.672$	$X = 0.390$, $Y = 0.152$, $Z = 1.29$							
	$a_{11} = 1$, $a_{12} = 2.41$	$a_{22} = 1$, $a_{21} = 0.58$							

Table 4 (continued)

No.	Isotherm Parameters K		Adsorption capacity, Qm (mg/g)				The goodness of fit (R^2)		Inference and Reference
			Single		Binary				
	1	2	1	2	1	2	1	2	
v)	$K_L = 6.65$	$K_L = 5.71$	0.22 meq/L	0.33 meq/L	0.26 – 0.24 meq/g	0.8 meq/L			Cd (II) adsorbed 1.3 times more than Zn(II) on sepiolite in a single-component adsorption system. In a competitive adsorption system, the behavior was different. Zn(II) presented assertive antagonistic behavior over Cd(II) adsorption. Cd(II) did not affect the adsorption of Zn(II). But the presence of Zn(II) reduced the uptake of Cd(II) up to 16.5 times due to the same cationic sites on the adsorbent (Padilla-Ortega et al. 2013)
	$K_F = 0.247$	$K_F = 0.279$							

Table 4 (continued)

No.	Isotherm Parameters K		Adsorption capacity, Qm (mg/g)				The goodness of fit (R^2)		Inference and Reference
			Single		Binary				
	1	2	1	2	1	2	1	2	
	K_{RP} = 570, α_{RP} = 2308, β = 0.680	K_{RP} = 4.86, α_{RP} = 14.8, β = 0.836			0, 0.2, 0.4, 0.8, 1 meq/L	0.32, 0.075, 0.042, 0.03, 0.02 meq/g			
	K_E = 107	K_E = 10.7							
	η = 0.088	η = 1.24							
	η = 0.584	η = 0.739							
	X = 1.105, Y = 0.105, Z = 1.13	X = 0.847, Y = 5.02, Z = 0.806							
	a_{11}=1, a_{12} =0.026	a_{22}=1, a_{21} =12.8							

Table 4 (continued)

No.	Isotherm Parameters K		Adsorption capacity, Qm (mg/g)				The goodness of fit (R²)		Inference and Reference
			Single		Binary				
	1	2	1	2	1	2	1	2	
vi)	$K_L = 0.256$	$K_L = 0.214$	94.33	86.20	88.14	70.12	0.997	0.987	Cd(II) has a better affinity than Ni(II) in a single-component system on maghemite nanotubes. In this study, the higher the pH value, the better the result. Cd(II) gets strongly influenced by Ni(II). (Roy and Bhattacharya 2013)
	$K_F = 11.15$	$K_F = 4.25$					0.881	0.860	

Table 4 (continued)

No.	Isotherm Parameters K		Adsorption capacity, Qm (mg/g)				The goodness of fit (R^2)		Inference and Reference
			Single		Binary				
	1	2	1	2	1	2	1	2	
vii)	$K_L = 0.105$	$K_L = 0.047$	86.20	60.60	65.62	58.83	0.991	0.989	Ni(II) absorbs more than Co(II) on γ-Fe2O3 nanotubes in a single adsorbent system. The adsorption effectivity from a single to a binary system has almost no change for Co(II). The higher the pH value, the better the adsorption shows in the study. (Roy and Bhattacharya 2013)
	$K_F = 4.42$	$K_F = 5.16$					0.891	0.912	

Table 4 (continued)

No.	Isotherm Parameters K		Adsorption capacity, Qm (mg/g)				The goodness of fit (R^2)		Inference and Reference
			Single		Binary				
	1	2	1	2	1	2	1	2	
viii)	$K_L = 0.059$	$K_L = 0.981$	60.60	94.33	55.87	85.27	0.981	0.986	Cd(II) adsorption success in a single-component system on maghemite nanotubes is higher than that of Co(II). Cd(II) adsorptions decrease firmly in Co(II) presence. The higher the pH value, the better the result in this study. (Roy and Bhattacharya 2013)
	$K_F = 5.66$	$K_F = 8.56$					0.941	0.856	

T temperature (°C), *D* Adsorbent Dosage (g/ml), *A* Agitation/speed (rpm), *CT* contact time (Mins), *SA* surface area, (m^2/g), *AC* Adsorption Capacity (mg/g), *Co* Initial concentration of adsorbates (mg/L), *Qm* The maximum adsorption capacity of a system (mg/g), *K* Isotherm adsorption constants, K_L, K_F, K_{RP}, η = factor of interactions for components of a system, n_L, n_{RP}, a
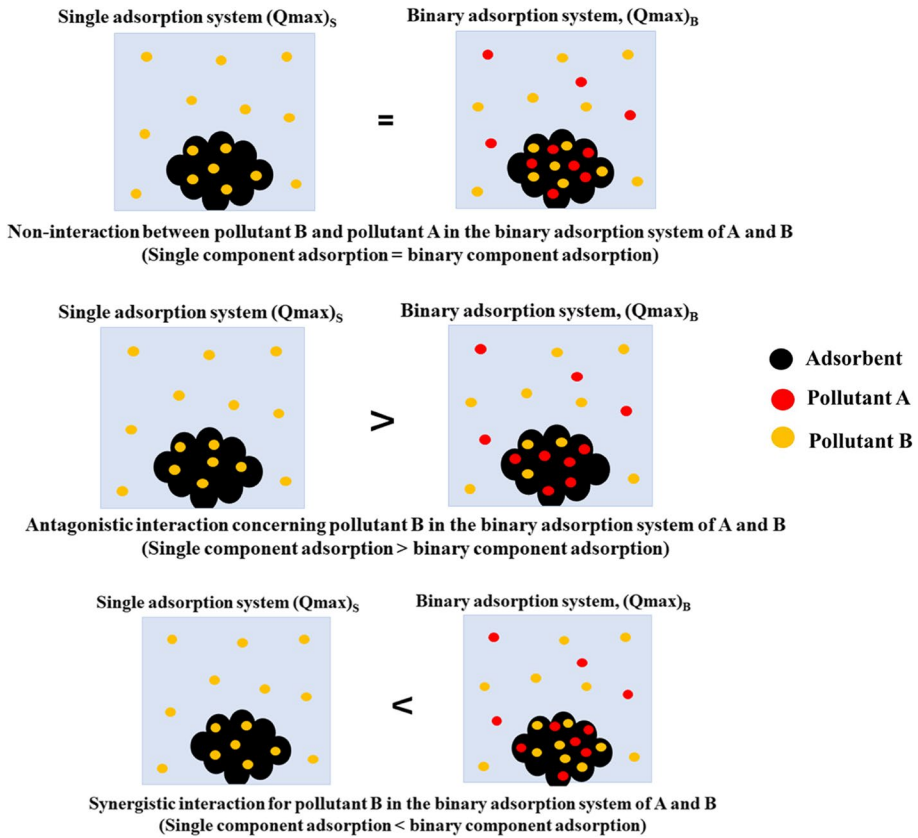
Fig. 6 Schematic representation of interaction mechanisms of pollutants in a competitive adsorption system

be compared, and it may be considered for correlation metric with hydrophobicity, van der Waals contacts, and molecular connectivity. Adsorption affinity is expressed by the equilibrium ratio of the solid-phase concentration to the liquid-phase concentration (Saikia and Dutta 2008). Table 5 lists the interaction mechanism for multi-component systems.

5 Modeling of Competitive Adsorption for Various Data

Modeling and simulation consist of performing a sensitivity analysis to ensure that the model parameter values are optimum. Initializing the model parameters with the smallest possible objective function value, such as the sum of square errors (SSE), is the first step in a sensitivity analysis. In the perturbation concept, one parameter is changed over time while the other parameters are held constant. Nonlinear regression analysis finds the best solution for minimizing errors and perturbation concepts. For each perturbation, the objective function is re-estimated, and later, a graph between a model parameter's percentage of perturbation and the accurate function value is drawn. The global minimum is reached if all model parameters are perturbed at 0%; otherwise, it represents a poor model (Mukhtar et al. 2020). In this investigation, the "solver add-in"

Table 5 Expressions of interaction mechanism of a binary system

No.	Interaction mechanism	Expression	References
1	Additive rule (AR)	$\sum_{j=1}^{2}(Q_S) = (Q_{i,S}) + (Q_{j,S})$ $\sum_{j=1}^{2}(Q_B) = (Q_{i,B}) + (Q_{j,B})$	Girish 2018
2	Selectivity ratio (S)	$S\left(i/j\right) = \dfrac{Q_{i,B}}{Q_{j,B}} = \dfrac{Q_{i,S}}{Q_{i,B}}$	Zhang et al. 2019
3	Relative percent Adsorption (R_Q)	$R_{Qi} = \dfrac{Q_{i,B}}{Q_{i,s}} X100$	Saǧ et al. 1998
4	Sorption Affinity (K_s)	$K_s = \dfrac{(C_{i,a})}{(C_{i,S})_B}$	Saikia and Dutta 2008
5	P-factor (P_{fi})	$P_{fi} = \dfrac{Q_{i,S}}{Q_{i,B}}$	Choy et al. 2004

$Q_{i,S}$ and $Q_{j,B}$ = single and binary component adsorption capacity of pollutant i and j, (mg/g); $C_{i,a}$ and $\left(C_{i,S}\right)_B$ = Initial concentration of component and solute in a solid phase in binary solution (mg/L)

in Microsoft Excel is employed for fitting and predicting the isotherm models. The adsorption constant 'K' values were found using the Excel Solver by maintaining the sum of squared errors between the actual experimental values 'Qe' and the predicted values 'Qe' model. The errors are minimized using the Excel Solver, and correlation coefficients R^2 are calculated. The comparison and the applicability of models for competitive adsorption are also learned.

In this study, the binary experimental data are taken from (Roy and Bhattacharya 2013). The single, binary, and ternary adsorption studies are carried out for cadmium, nickel, and cobalt using maghemite γ-Fe_2O_3 nanotubes as adsorbents. The extrapolated experimental data set is modeled using a few isotherm models, shown in Table 3. Roy and Bhattacharya (2013) presented the fit of the Langmuir and Freundlich isotherm model for the mono-component adsorption system and under the experimental conditions V = 100 mL, Co = 20 to 400 mg/L, pH = 6 ± 0.1, adsorbent dosage = 0.05 g, T = 30 °C, shaking time = 4 h. A binary combination of cadmium-nickel, nickel–cobalt, and cadmium-cobalt was considered with an equal concentration ratio of 1:1 (Roy and Bhattacharya 2013). The analysis focuses on interpreting the behavior of the interaction between the adsorbent and adsorbate, the adsorption scenario of isotherm models, and the prediction of isotherm models (Qu et al. 2020).

This study uses extrapolated data from Roy and Bhattacharya (2013) for modeling and simulation by four multi-component adsorption isotherm models. The isotherms such as the Modified Competitive Langmuir (MCL) isotherm model (Sohn and Kim 2005), Extended Langmuir Isotherm model (Srivastava and Tyagi 1995), Langmuir–Freundlich isotherm model (Costa et al. 2019), and Extended Freundlich isotherm model (Girish 2019) are used to fit experimental data obtained for cadmium-nickel, nickel–cobalt, and cadmium-cobalt. These models can determine competitive equilibrium, maximum adsorption capacity, and affinity parameters. They are based on nonlinear equation forms instead of linear forms, and the prediction of multi-component adsorption is initialized.

6 Modeling Results

6.1 Competitive Adsorption Isotherms of Cadmium-Nickel

Experimental data from Roy and Bhattacharya (2013) were used in multi-component adsorption modeling. Multi-component models were fitted using MS Excel Solver by
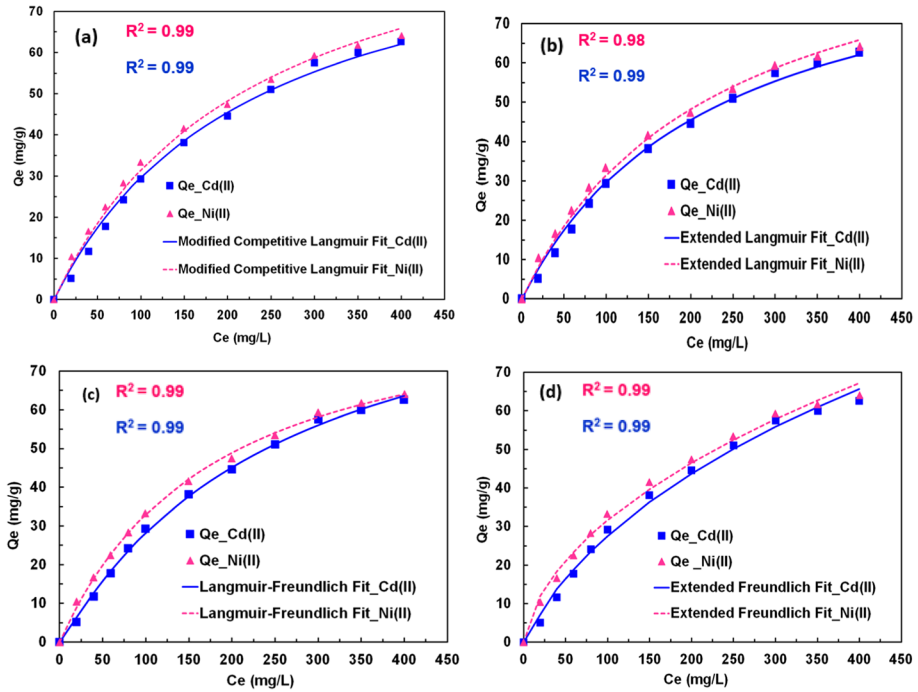
Fig. 7 **a** Modified Competitive Langmuir Isotherm, **b** Extended Langmuir Isotherm, **c** Langmuir–Freundlich Isotherm, and **d** Extended Freundlich Isotherm model fit of competitive adsorption of Cd(II) and Ni(II)

minimizing least square errors. Figure 7a shows the Modified Competitive Langmuir (MCL) isotherm model fit of adsorption of Cd(II) and Ni(II). The actual experimental values Qe and the predicted values Qe model (Fig. 7a) are plotted against the equilibrium concentration Ce, and the graph presents the fitted line and R^2. The Modified Competitive Langmuir (MCL) isotherm model equation exhibited fit with a correlation coefficient of 0.99 and 0.99 for Cd(II) and Ni(II), respectively, with minimized errors. The maximum adsorption capacities of the adsorption system were 207.77 mg/g and 196.09 mg/g for Cd(II) and Ni(II), respectively. The high R^2 values suggest a good fit in the adsorption system for Cd(II) and Ni(II). The fit is good if the R^2 value is greater than 0.95. The K values reflect the affinity of maghemite γ-Fe_2O_3 nanotubes towards Cd(II) and Ni(II) in the binary system and are 0.022 L/mg and 0.033 L/mg, respectively.

Figure 7b shows the Extended Langmuir Isotherm/Non-modified Langmuir (EL) isotherm model fit of adsorption of Cd(II) and Ni(II). The Qe and Qe model (Fig. 7b) was plotted against the equilibrium concentration Ce, and the graph presents the fitted line equation and R^2. The Extended Langmuir Isotherm/ Non-modified Langmuir (EL) isotherm model equation exhibited good fit with R^2 values of 0.98 and 0.99 for Cd(II) and Ni(II), respectively, with minimized errors. The maximum uptake of the system was 203.63 mg/g, and 199.06 mg/g for Cd(II) and Ni(II), respectively. In the binary system, K values reflect the affinity of maghemite γ-Fe_2O_3 nanotubes for cadmium (0.0021 L/mg) and nickel (0.0022 L/mg).

Figure 7c shows the Langmuir–Freundlich isotherm model fit of Cd(II) and Ni(II) adsorption. The graphs present Qe and Qe model plotted against the equilibrium concentration Ce, and show the fitted line equation and R^2 (Fig. 7c). The Langmuir–Freundlich isotherm model exhibited fit with R^2 values of 0.99 and 0.99 for Cd(II) and Ni(II), respectively, with minimized errors. The maximum adsorption capacities of the adsorption system were 195.54 mg/g and 191.49 mg/g for Cd(II) and Ni(II), with K values of 0.0014 and 0.0027 $(mg/g)/(mg/L)^{1/n}$, respectively.

Figure 7d shows the Extended Freundlich isotherm model fit of adsorption of Cd(II) and Ni(II). The Qe and Qe model (Fig. 7d) was plotted against the equilibrium concentration Ce, and the graph presents the fitted line equation and R^2. The Extended Freundlich Isotherm model equation exhibited an excellent fit with R^2 values of 0.99 and 0.99 for cadmium and nickel, respectively, with minimized errors.

6.2 Competitive Adsorption Isotherms of Cadmium-Cobalt

Experimental data from Roy and Bhattacharya (2013) were taken for multi-component adsorption modeling. Multi-component models were fitted using Excel Solver by minimizing least square errors. Figure 8a shows the Modified Competitive Langmuir (MCL) isotherm model fit of adsorption of cadmium and cobalt. The Qe and Qe model (Fig. 8a) was plotted against the equilibrium concentration Ce, and the graph presents the fitted line equation and R^2. The Modified Competitive Langmuir (MCL) isotherm model equation exhibited fit with R^2 values of 0.95 and 0.94 for cadmium and cobalt, respectively, with minimized errors. The maximum adsorption capacities of the adsorption system were 200.20 mg/g and 205.87 mg/g for Cd(II) and Co(II), respectively. In the binary system, the K values of Cd(II) (0.028 L/mg) and Co(II) (0.027 L/mg) reflect the affinity towards maghemite γ-Fe_2O_3 nanotubes.

Figure 8b shows the Extended Langmuir/Non-modified Langmuir (EL) isotherm model fit of adsorption of Cd(II) and Co(II). The actual experimental values Qe and the predicted values Qe model (Fig. 8b) were plotted against the equilibrium concentration Ce, and the graph presents the fitted line equation and R^2. The Extended Langmuir Isotherm/ Non-modified Langmuir (EL) isotherm model equation exhibited fit with correlation coefficient values of 0.95 and 0.94 for Cd(II) and Co(II), respectively, with minimized errors. The maximum adsorption capacities of the adsorption system were 199.64 and 206.42 mg/g for Cd(II) and Co(II), respectively. Cadmium and cobalt affinities to maghemite γ-Fe_2O_3 nanotubes were 0.0046 and 0.0047 L/mg, respectively.

Figure 8c shows the Langmuir–Freundlich isotherm model fit of adsorption of Cd(II) and Co(II). The graph consists of the Qe and Qe model plotted against the equilibrium concentration Ce, and the graph presents the fitted line equation and R^2 (Fig. 8c). The Langmuir–Freundlich isotherm model exhibited satisfactory fit with an R^2 values of 0.97 and 0.96 for Cd(II) and Co(II), respectively, with minimized errors. The maximum uptake of this system was 189.20 mg/g and 209.74 mg/g, and the K values were 0.0028 and 0.0060 $(mg/g)/(mg/L)^{1/n}$ for cadmium and cobalt, respectively.

Figure 8d shows the Extended Freundlich isotherm model fit of adsorption of Cd(II) and Co(II). The actual experimental values Qe and the predicted values Qe model (Fig. 8d) were plotted against the equilibrium concentration Ce, and the graph presents the fitted line equation and R^2. The Extended Freundlich Isotherm model equation exhibited good fit with R^2 values of 0.96 and 0.98 for cadmium and cobalt, respectively, with minimized errors.
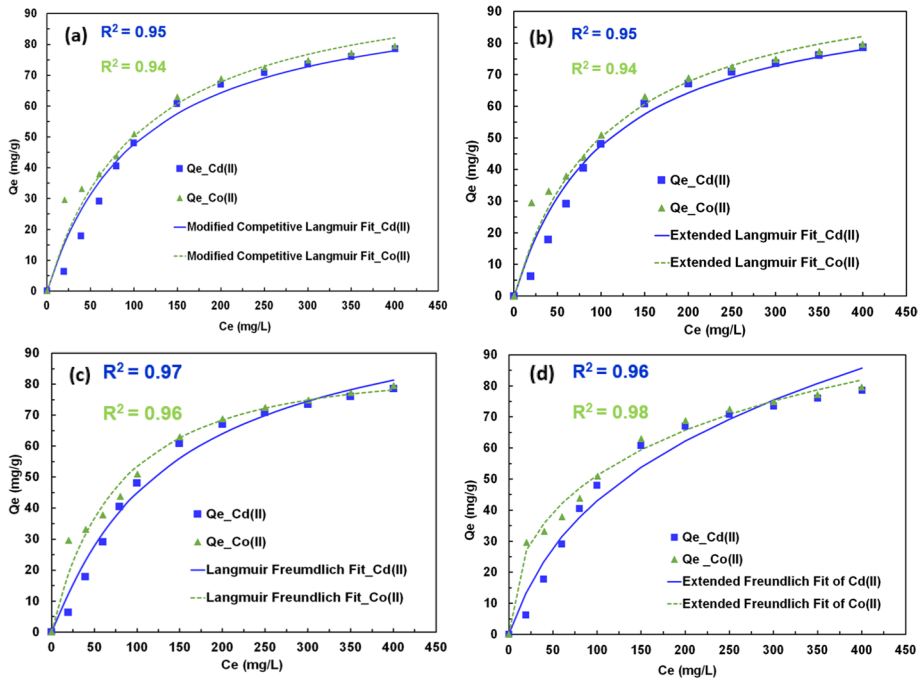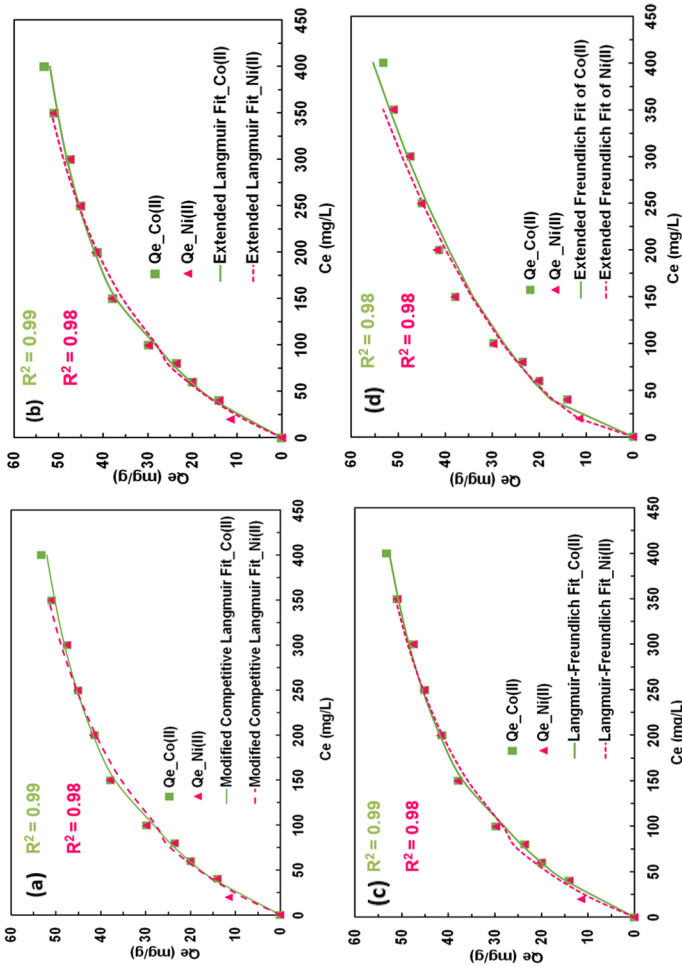
Fig. 8 **a** Modified Competitive Langmuir Isotherm, **b** Extended Langmuir Isotherm, **c** Langmuir–Freundlich Isotherm model, and **d** Extended Freundlich Isotherm model fit of competitive adsorption of Cd(II) and Co(II)

6.3 Competitive Adsorption Isotherms of Nickel–Cobalt

Experimental data from Roy and Bhattacharya (2013) was taken for multi-component adsorption modeling. Multi-component models were fitted using the Excel Solver by minimizing the least square errors. Figure 9a shows the Modified Competitive Langmuir (MCL) isotherm model fit of adsorption of nickel and cobalt. The Qe and Qe model (Fig. 9a) was plotted against the equilibrium concentration Ce, and the graph presents the fitted line equation and R^2. The Modified Competitive Langmuir (MCL) isotherm model equation exhibited fit with R^2 values of 0.98 and 0.99 for nickel and cobalt, respectively, with minimized errors. The maximum adsorption capacities of the adsorption system were 176.01 and 124.93 mg/g for Ni(II) and Co(II), respectively. In the binary system, the K values of Ni(II) (0.018 L/mg) and Co(II) (0.032 L/mg) reflect the affinity towards maghemite γ-Fe$_2$O$_3$ nanotubes.

Figure 9b shows the Extended Langmuir Isotherm/Non-modified Langmuir (EL) isotherm model fit of adsorption of nickel and cobalt. The Qe and Qe model (Fig. 9b) was plotted against the equilibrium concentration Ce, and the graph presents the fitted line equation and R^2. The Extended Langmuir Isotherm/ Non-modified Langmuir (EL) isotherm model equation exhibited fit with R^2 values of 0.98 and 0.99 for nickel and cobalt, respectively, with minimized errors. The maximum adsorption capacities of the system were 147.21 and 144.61 mg/g for Ni(II) and Co(II), respectively. The

Fig. 9 **a** Modified Competitive Langmuir Isotherm, **b** Extended Langmuir Isotherm, **c** Langmuir–Freundlich Isotherm, and **d** Extended Freundlich Isotherm model fit of competitive adsorption of Ni(II) and Co(II)

high R^2 value indicates a good fit in the adsorption system for nickel and cobalt. In this binary system, the K values reflect the affinities of maghemite γ-Fe$_2$O$_3$ nanotubes towards Ni(II) and Co(II), which were 0.0034 L/mg and 0.0031 L/mg, respectively.

Figure 9c shows the Langmuir–Freundlich isotherm model fit of adsorption of Ni(II) and Co(II). The graph presents Qe and Qe model plotted against the equilibrium concentration Ce, and the graph presents the fitted line equation and R^2 (Fig. 9c). The Langmuir–Freundlich isotherm model exhibited fit with R^2 values of 0.98 and 0.99 for nickel and cobalt, respectively, with minimized errors. The maximum adsorption capacities of the adsorption system were 165.13 mg/g and 134.10 mg/g, and K values were 0.0034 and 0.0032 (mg/g)/(mg/L)$^{1/n}$ for Ni(II) and Co(II), respectively.

Figure 9d shows the Extended Freundlich Isotherm model fit of adsorption of Ni(II) and Co(II). The Qe and Qe model (Fig. 9d) is plotted against the equilibrium concentration Ce, and the graph presents the fitted line equation and R^2. The Extended Freundlich Isotherm model equation exhibited fit with R^2 values of 0.98 and 0.98 for Ni(II) and Co(II), respectively, with minimized errors.

The four multi-component isotherm models modeled the binary adsorption system for cadmium-nickel, nickel–cobalt, and cadmium-cobalt. The isotherms such as the Modified Competitive Langmuir (MCL) isotherm model (Sohn and Kim 2005), Extended Langmuir Isotherm model (Srivastava and Tyagi 1995), Langmuir–Freundlich isotherm model (Costa et al. 2019), and Extended Freundlich isotherm model (Girish 2019) are modeled with the equations given in Table 3. As indicated in Table 6, the parameters are predicted using non-linearized equations by reducing errors. In this binary system of Cd(II)-Ni(II), the maximum uptake is by Cd(II), and the maghemite γ-Fe$_2$O$_3$ nanotubes have more affinity towards the Cd(II) than Ni(II), as in Table 4. The inferences of modeling studies of pollutants are given in Table 7. Similarly, in the competitive system of Ni(II)-Co(II) and Cd(II)-Co(II), Ni(II) adsorbed more than Co(II), and Co(II) uptakes more than Cd(II), respectively. The findings show that adsorption behavior in binary component systems is complicated, as it is expected. Metal ion uptake and characteristics are thought to be related by many parameters (Manning and Goldberg 1996). Competitive adsorption is caused by factors such as electronegativity of the Ni(II), Co(II), and Cd(II) which is 1.91, 1.88, and 1.69, respectively. Similarly, electrostatic attrition is caused by the charge-to-radius ratio, capacity to form metal hydroxide complex, and appropriate active site for adsorption on the adsorbent (Kong et al. 2020). The hydrated radii of Ni(II), Co(II), and Cd(II) are 4.04 Å, 4.23 Å, and 4.26 Å, respectively (Roy and Bhattacharya 2013). As a result, Ni(II) has a better probability than Co(II) and Cd(II) of accessing active sites and pores more quickly. Ionic radii of Ni(II), Co(II), and Cd(II) are 0.69 Å, 0.745 Å, and 0.97 Å, respectively. The adsorption rate decreases as the ionic radius increases (Mustafa et al. 2013). All four competitive isotherm models gave a good fit, as shown by the R^2 values. This indicates that several isotherms may provide a good fit for multi-component isotherms. However, parameters from single-component systems cannot be directly used to model multi-component systems. Cd(II) exhibits a higher affinity in a single-component solution than Ni(II) for maghemite nanotubes. In a single-component solution, the success of Cd(II) adsorption on maghemite nanotubes is higher than that of Co(II). When Co(II) is present, Cd(II) adsorptions are strongly reduced. On γ-Fe$_2$O$_3$ nanotubes, Ni(II) absorbs more than Co(II) in a single adsorbent system. In a binary system, Co(II) adsorption effectivity changes.

Table 6 Modeling results of adsorption in the binary system of pollutants

Binary system	Isotherm models																	
	Modified competitive Langmuir				Extended Langmuir			Langmuir–Freundlich				Extended Freundlich						
	Q_m (mg/g)	K (L/mg)	η	R^2	Q_m (mg/g)	K (L/mg)	R^2	Q_m (mg/g)	K $(mg/g)/(mg/L)^{1/n}$	n	R^2	K_F $(mg/g)/(mg/L)^{1/n}$	n	x	y	z	R^2
Cd(II) and Ni(II)	207.77	0.022	10.80	0.99	203.63	0.0021	0.98	195.54	0.0014	0.916	0.99	12.24	2.91	4.21	26.49	3.53	0.99
	196.09	0.033	14.62	0.99	199.06	0.0022	0.99	191.49	0.0027	1.017	0.99	6.36	2.31	0.42	3.31	0.002	0.99
Cd(II) and Co(II)	200.20	0.028	6.23	0.95	199.64	0.0046	0.95	189.20	0.0028	0.900	0.97	12.24	2.91	1.74	18.51	0.901	0.96
	205.87	0.027	5.91	0.94	206.42	0.0047	0.94	209.74	0.0060	1.042	0.96	7.94	2.42	1.25	0.0004	2.22	0.98
Co(II) and Ni(II)	124.93	0.032	9.08	0.99	144.61	0.0031	0.99	134.10	0.0032	0.995	0.99	7.74	2.42	0.28	2.46	0.073	0.98
	176.01	0.018	6.23	0.98	147.21	0.0034	0.98	165.13	0.0034	1.027	0.98	6.36	2.31	0.23	1.98	0.001	0.98

Table 7 Inferences of modeling studies of pollutants

No.	Heavy metals	Adsorbent	Competitive isotherm models	Competitive modeling inferences
(i)	Cd(II) and Ni(II)	Maghemite γ-Fe$_2$O$_3$ nanotubes	1. Modified Competitive Langmuir isotherm model 2. Extended Langmuir Isotherm model 3. Langmuir–Freundlich isotherm model and 4. Extended Freundlich isotherm model	Cd(II) exhibits a higher affinity in a single-component solution than Ni(II) for maghemite nanotubes. In this case study, the adsorption of Cd(II) is higher if the pH value is higher. The presence of Ni(II) has a significant antagonistic impact on Cd(II) adsorption. The highest absorption in this binary system of Cd(II)-Ni(II) is by Cd(II), and maghemite γ-Fe$_2$O$_3$ nanotubes have a stronger affinity for Cd(II) than Ni(II)
(ii)	Cd(II) and Co(II)			In a single-component solution, the adsorption capacity of Cd(II) on maghemite nanotubes is higher than that of Co(II). When Co(II) is present, Cd(II) adsorption is strongly reduced. In this investigation, better adsorption results were obtained at higher pH values. Similar to this, Co(II) uptake exceeded Cd(II) uptake in the competitive system of Cd(II)-Co(II).
(iii)	Co(II) and Ni(II)			Ni(II) adsorption is more than Co(II) adsorption in a single adsorbent system. In a binary system, Co(II) adsorption capacity reduces. The study shows that adsorption results are better at higher pH values. In the Ni(II)-Co(II) competitive system, Ni(II) adsorption was more than Co(II).

7 Discussion

Many of the contaminants are found to occur simultaneously in nature. For example, arsenic and fluoride, lead and zinc, vanadium and chromium, zinc and nickel, cadmium and zinc are co-occurring in groundwater. In the case study of Cd(II)-Ni(II) that we considered for modeling, Cd(II) showed a higher affinity than Ni(II). Similarly in the competitive adsorption systems of Ni(II)-Co(II) and Cd(II)-Co(II), Ni(II) adsorption was more than Co(II) adsorption, and Co(II) adsorption was more than Cd(II), respectively. Overall, in any multi-component adsorption system, presence of one contaminant in the solution can impact the adsorption of other pollutants. For instance, arsenic shows antagonistic behavior with fluoride during simultaneous adsorption. Zinc is also known to show intense antagonism in the presence of nickel. Identifying the behaviors of synergistic, antagonistic, and no- interaction of contaminants is possible by experimental studies and from inferences of previous research papers. The intricacy of competitive adsorption depends on several variables, like the competition to reach the active sites of the adsorbent surface, the component ionic radii and their bonding. Surface charge of the adsorbent will vary with the pH of the solution. The concentration of a particular hydrated specie will also change with the pH and with the concentration of other ions. Hence, pH will influence the adsorption significantly. When one component's concentration rises, another component's adsorption reduces, and interaction between the species in the solution determines how

one component influences another (Roy and Bhattacharya 2013). The displacement effect, a changed adsorbent surface, and the addition of extra components to inhibit the active sites can change how adsorbent and adsorbate interact (Girish 2018). Multi-component adsorption equilibrium systems are dependent on the functional group, structure, shape, and size of adsorbents, the electrostatic force of attraction for adsorption, the capacity to generate hydroxides, the ionic characteristics of pollutants, the hydrated radii, molecular weight, and the size of adsorbates.

The multi-component isotherm models are primarily based on assumptions and experimental conditions for interference and competition. The behavior of the Langmuir and Freundlich isotherms are combined in the Non-Modified Competitive Redlich Peterson Isotherm model. In some cases, this model behaves as both models. An extra-term interaction component is introduced into the Modified Competitive Redlich Peterson Isotherm model to better describe the competitiveness between the adsorbents and adsorbates. An enhanced version of the Jain-Snoeyink model, the modified Jain-Snoeyink Isotherm model includes the interaction term in the equation (Sheng et al. 2007). Under these conditions, a component's maximal adsorption capacity must be more significant than its counterpart. The Steric Mass Action Isotherm Model aims to adsorb proteins (Russell and Carta 2005). It was first applied to single-component adsorption, and then, it was further employed for multi-component adsorption, which proved ineffective. Other isotherm models have since been explicitly used in appropriate adsorption systems.

The specific equilibrium condition, the maximum adsorption (q_{max}), the concentration of molecules (C), the interaction factor (η) which depicts the competitive impact of adsorbates in the solution, and K which denotes the Langmuir constant for components are evaluated from the experimental data in the modified competitive Langmuir isotherm model. In the extended Langmuir isotherm model, the adsorbates have a non-interacting effect. The last assumption is that the pollutant molecules adsorb on the active sites. The drawback of this model is that the values of the isotherm parameters for various adsorbents might be drastically different. The formula has the same variables as the modified competitive Langmuir isotherm model without the interaction factor. A disadvantage of the extended Freundlich isotherm model is that additional fitting parameters are required for a binary system. The parameters K and n describe the isotherm constants for components, C is the concentration of components in an aqueous solution at equilibrium, and x, y, and z express the isotherm constants for components. The Langmuir–Freundlich isotherm model is a combination of Freundlich and Langmuir isotherm models. It could be possible to get better outcomes by merging the two models. The Langmuir–Freundlich model is generated with all parameters based on multi-component equilibrium data. The parameter K_{LF} defines the intensity of adsorbent and adsorbate interactions, and n represents the heterogeneity and favorability.

Though widely used, adsorption isotherm models are black box type models that do not consider the mechanisms of adsorption. Adsorption isotherm models give good predictions for single-component adsorption systems, but they are unable to capture the complexities of multi-component systems. The limitations of a multi-component adsorption models are that they are unable to predict the interactions of different components (such as synergistic effects) and competitive effects. Most isotherm models cannot explain the competitive characteristics in multi-component adsorption systems, such as preferential adsorption, antagonism, and synergistic adsorption. Model parameters from single-component isotherms systems such as Langmuir and Freundlich cannot be used in multi-component systems, even for similar systems. Additionally, intrinsic adsorption heterogeneity becomes more complicated if the adsorbent is microporous (Jadhav and Srivastava 2019). Factors

such as surface charge, structure, size, functional groups of the component, porosity and active sites on the adsorbent surface affect the components to each other in a system. Surface complexation modeling is a complicated method that can be used to determine multi-component adsorption surface reaction mechanisms (Jeppu and Clement 2012). However, the Log K values have to be determined for each system. It is essential to understand the effects of aqueous complexation between metals and ligands and the impact of surface charge change on adsorption owing to differences in solution ionic strength (Gun'ko 2007). Multi-component equilibrium adsorption takes account of a constant separation factor when one or several components are poorly adsorbed (Girish 2018). The pH of each isotherm is intended to remain constant, since pH is crucial to the adsorption system. No pH-dependent multi-component isotherm model systems exist (Pereira et al. 2023). Finding a suitable model for the competitive adsorption behavior of a component mixture is challenging since most existing non-linear models rely heavily on single-component data (Zhu et al. 1991).

8 Conclusions

Though there are several drinking water contaminants such as arsenic and fluoride, which are known to occur simultaneously in nature, there is inadequate research on multi-component isotherm models for predicting simultaneous adsorption systems. In this review paper, models of multi-component systems were compiled, and case studies were considered. Several multi-component adsorption isotherms and competitive mechanisms and constraints were analyzed. Numerous adsorption models, including the Henry isotherm model, Langmuir isotherm model, Freundlich isotherm model, Langmuir Freundlich hybrid, Brunauer-Emmett-Teller, Modified Competitive Langmuir, Langmuir Extension First Approximation Model, Freundlich-Langmuir-Jovanovic, Modified Langmuir Freundlich, LeVan-Vermeulen model, were reviewed along with their equations and significance. The equations, parameters, and relevance of each isotherm model are summarized in this paper in Table 2 and Table 3.

In this study, the competitive adsorption of commonly found multi-component contaminant adsorption systems of cadmium-nickel, nickel–cobalt, and cadmium-cobalt is considered and predicted using the various multi-component adsorption models such as Modified Competitive Langmuir (MCL), Extended Langmuir Isotherm (EL) model, Langmuir–Freundlich isotherm model, and Extended Freundlich Isotherm model (Table 6). The adsorbent in the multi-component system of Cd(II)-Ni(II) showed a higher affinity for Cd(II) than Ni(II), with a maximum absorption of 207.77 mg/g by Cd(II). Similarly, in the competitive adsorption of Ni(II)-Co(II) and Cd(II)-Co(II), Ni(II) adsorption was 176.01 mg/g, which is more than Co(II) adsorption, and Co(II) absorbed 205.87 mg/g, which is more than Cd(II), respectively. This suggests that some components are preferably adsorbed over others. The reasons for preferable adsorption and antagonism have to be further researched. The prediction of multi-component adsorption was done using isotherm models. Microsoft Excel Solver was used to determine the equilibrium systems' maximum adsorption capacity (Q_m) and parameters such as K, n, and η using the MS Excel Solver addin. The multi-component isotherm models provided a good fit as suggested by the coefficient of determination (R^2) values. This suggests that several multi-component isotherms can provide a good fit for simultaneous adsorption experimental data though they do not consider the mechanism of adsorption, if they are fit for each dataset seperately.

Theoretical adsorption isotherm models are important for designing treatment plants, filtering units, and packed bed column studies. The knowledge of competitive isotherm models is needed in the design of multi-component adsorption and treatment systems. Current multi-component isotherm models are unable to represent the interactions of various components such as synergistic, antagonistic and competitive effects. Further advanced research is also required to elucidate the multi-component interaction mechanisms and competitive adsorption mechanisms at the surface, ionic and molecular level. Moreover, currently none of the multi-component isotherms are able to model adsorption under different pH conditions. So, further investigation has to be done to develop new equations for multi-component adsorption of co-occurring contaminants to overcome the above limitations.

Nomenclature

HI: **Henry isotherm Model;** Q_e : **Equilibrium adsorption capacity of adsorbents, (mg/g);** C_e : **Equilibrium concentration of adsorbates, (mg/L);** C_0 : **Initial concentration of adsorbates, (mg/L);** K_{H_e} : **Henry constant, (cm^3/g);** *LI*: **Langmuir isotherm model;** Q_m : **Maximum adsorption capacity of adsorbent, (mg/g);** k_L : **Langmuir constant, (L/mg);** *FI*: **Freundlich isotherm model;** K_F : **Freundlich constant, (L/mg);** BET: **Brunauer, Emmett, Teller isotherm model;** C_S : **Saturated solute concentration, (mg/L);** *T model*: **Toth Model;** K_T : **Toth Equilibrium constant, (L/mg);** a_T : **Affinity co-efficient dependent on temperature;** *RPI*: **Redlich Peterson Isotherm model;** $k_{RP}, \alpha_{RP}, \beta$: **Redlich Peterson constants;** *MLF*: **Modified Langmuir Freundlich isotherm model;** k_a : **Affinity co-efficient for adsorption, (L/mg);** *ELI*: **Extended Langmuir isotherm model;** $Q_{e,i}$: **Equilibrium adsorption capacity for component** *i,* **(mg/g);** $Q_{m,i}$: **Maximum adsorption capacity for component** *i,* **(mg/g);** $K_{L,i}$: **Langmuir constant for component** *i,* **(L/mg);** $K_{L,j}$: **Langmuir constant for component** *j,* **(L/mg);** $c_{e,i}$: **Equilibrium concentration for component** *i,* **(mg/L);** $c_{e,j}$: **Equilibrium concentration for component** *j,* **(mg/L);** *LEFA*: **Langmuir Extension First Approximation model;** $A_i \& B_i$: **Single solute parameter of component** *i;* $A_j \& B_j$: **Single solute parameter of component** *j;* $A_{ij} \& B_{ij}$: **Interaction factor between two components** *i & j* **in a solution;** *EF*: **Extended Freundlich isotherm model;** $K_{F,i}$: **Freundlich constant for component** *i,* **(L/mg);** $K_{F,j}$: **Freundlich constant for component** *j,* **(L/mg);** $n_i \& n_j$: **Adsorption intensity for components** *i & j* **in a solution;** $x_i \& x_j$: **Experimental constant values of plot** $Q_{e,i}$ **vs** $C_{e,i}$ **;** $y_i \& y_j$: **Experimental constant values of plot** $Q_{e,j}$ **vs** $C_{e,j}$ **;** $z_i \& z_j$: **Experimental constant values of plot** $Q_{e,i}$ **vs** $C_{e,i}$ **;** *NMCRP*: **Non-Modified Competitive Redlich Peterson Isotherm;** $K_{RP,i}$: **Redlich Peterson constant for component** *i,* **(L/mg);** *SRS*: **Sheindorf Rebuhn Sheintuch isotherm model;** a_{ij} : **Interaction factor between two components** *i & j* **in a solution;** *ES*: **Extended Sips Isotherm;** $K_{s,i}$: **Sips constant for components** *i,* **(L/mg)** ^{m} **; JS: Jain- Snoeyink model;** $Q_{maxi} \& Q_{maxj}$: **Maximum adsorption capacity for component** *i & j,* **(mg/g);** $K_i \& K_j$: **Jain Snoeyink constant for component** *i & j,* **(L/mg);** *MJS*: **Modified Jain- Snoeyink model;** $Q^0_{maxi} \& Q^0_{maxj}$: **Monolayer saturation capacity of Langmuir model for component** *i & j,* **(mg/g) or Single component data;** Q_{maxj} : **Maximum adsorption capacity for component** *j* **competitive with** *I,* **(mg/g);** *SMA*: **Steric Mass Action isotherm model;** C_{eq} : **Equilibrium concentration of liquid protein, (mg/L);** Q_0 : **Concentration of charged ligands in stationary stage, (mg/g);** K_i : **Equilibrium constant for component** *I;* $z_i \& z_j$: **Effective charge on protein for component** *I & j;* *FLJ*: **Freundlich-Langmuir- Jovanovic isotherm model;** C_{eq} : **Equilibrium concentration of liquid protein, (mg/L);** A_i : **Empirical constant;** *LV*: **Levan–Vermeulen model;** $K_i \& K_j$: **Affinity constants between the components** *i & j;* *EBEF*: **Empirical Bisolute Extension of the Freundlich Isotherm model;**

$Y_i \& Y_j$: **Equilibrium adsorption capacity of adsorbents i & j, (mg/g);** $X_i \& X_j$: **Equilibrium concentration of components i & j, (mg/L);** $a_i = K_i \& a_j = K_j$: **Freundlich constant for the components i & j;** $a_{ij}, a_{ji}, b_{ij}, b_{ji}$: **Interaction parameters obtained from Experimental values.;** *IASFC*: **Ideal Adsorbed Solution Theory Freundlich Isotherm model;** $K_i \& K_j$: **Freundlich constant for the components i & j;** $n_i \& n_j$: **Adsorption intensity for components i & j in a solution;** *SIAS*: **Simplified Ideal Adsorbed Solution Isotherm model;** K' : **Average values of k_i & k_j for components i & j in a solution;** n' : **Average values of n_i & n_j for components i & j in a solution;** K_i : **Freundlich constant for single component i, (L/mg);** n_i : **Adsorption intensity for single component i;** *ISIAS*: **Improved Simplified Ideal Adsorbed Solution Isotherm model;** K_i : **Freundlich constant for single component i, (L/mg);** n_i : **Adsorption intensity for single component i;** *IAS*: **Ideal Adsorbed Solution Model;** $Q_{e,i}^0$: **Concentration loading of solid phase, (mg/g);** C_i^0 : **Concentration for single solute i, (mg/L);** z_i : **Mole fraction in Adsorbed phase of i;** X_i : **Free mole fraction in liquid-solvent phase of i;** C_T : **Total concentration of all solutes in liquid phase, (mg/L);** *PPT*: **Polanyi's Potential theory Model;** P_S : **Saturation Pressure, (kPa);** *S model*: **Solubility normalized model;** C_S : **Solubility of adsorbate in a solvent, (mg/L);** $v_A \& v_T$: **Molar volumes of Asphaltenes and Toluene, (m³/mol);** *MPP*: **Modified Polanyi potential isotherm;** C^0 : **Standard concentration of the solution, (mol/dm³);** *DA Model*: **Dubinin Astakhov isotherm Model;** N_{ads} : **Equilibrium adsorption capacity, (mg/g);** $N_{ads,max}$: **Maximum adsorption capacity, (mg/g)**

Greek Symbols

SP: **Sips model;** β_s : **Sips model exponential;** *RPI*: **Redlich Peterson Isotherm model;** $k_{RP}, \alpha_{RP}, \beta$: **Redlich Peterson constants;** *MCL*: **Modified Competitive Langmuir Isotherm model;** $\eta_{L,i}$: **Interaction Factor dependent on concentrations of components i & j;** *NMCRP*: **Non-Modified Competitive Redlich Peterson Isotherm;** $\alpha_{RP,j}$: **Model constant for component j, (L/mg);** β, j : **Exponent varying from 0 & 1;** *MCRP*: **Modified Competitive Redlich Peterson Isotherm;** $\eta_{RP,i} \& \eta_{RP,j}$: **Factor of interactions for components i & j in a solution;** *SMA*: **Steric Mass Action isotherm model;** σ_S : **Steric hinderance;** c_{cl^-} : **Concentration of Chloride ion/ counter ion (mM);** *FLJ*: **Freundlich-Langmuir- Jovanovic isotherm model;** $\wedge$: **Maximum protein binding capacity;** α_i : **Exponential term for component i;** *EBEF*: **Empirical Bisolute Extension of the Freundlich Isotherm model;** $a_i = K_i \& a_j = K_j$: **Freundlich constant for the components i & j;** $a_{ij}, a_{ji}, b_{ij}, b_{ji}$: **Interaction parameters obtained from Experimental values.;** *ISIAS*: **Improved Simplified Ideal Adsorbed Solution Isotherm model;** η : **Co-efficient of competition or solubility factor;** n_i : **Adsorption intensity for single component i;** *S model*: **Solubility normalized model;** $\delta_A \& \delta_T$: **Solubility parameters of Asphaltenes and Toluene;** *DR Model*: **Dubinin Radushkevitch isotherm model;** β : **Adsorption free energy constant, (mol²/J²);** ε : **Polanyi/ adsorption Potential, (J/mol)**

Subscripts

FI: **Freundlich isotherm model;** n : **Adsorption intensity;** *LFHI*: **Langmuir Freundlich hybrid isotherm model;** m : **Factor of heterogeneity;** *BET*: **Brunauer, Emmett, Teller isotherm model;** B: **Interaction with the surface pertaining to BET constant;** *T model*: **Toth Model;** t: **Fitting parameter;** *MLF*: **Modified Langmuir Freundlich isotherm model;** n: **Heterogeneity index;** *ELI*: **Extended Langmuir isotherm model;** N: **Number of components in a solution;** *ES*: **Extended Sips Isotherm;** m : **Exponent varying from 0 & 1;** *SMA*: **Steric Mass Action isotherm model;** Q : **Equilibrium concentration of protein adsorption, (mg/L);**

FLJ: **Freundlich-Langmuir- Jovanovic isotherm model;** Q : **Equilibrium concentration of protein adsorption, (mg/L);** *IASFF*: **Ideal Adsorbed Solution Theory Freundlich model;** K : **Concentration range for** $a_{i,k} and b_{i,k}$ **is valid as numerical index;** C : **Integration constant value for integral spreading pressure, (mmol/g);** X : **Concentration of Liquid-phase, (mmol/L);** Y : **Carbon loading, (mmol/g);** z : **Mole fraction of absorbed phase;** *IAS*: **Ideal Adsorbed Solution Model;** R : **Ideal gas constant;** T : **Absolute temperature;** A : **Adsorbent surface area;** *PPT*: **Polanyi's Potential theory Model;** R : **Universal ideal gas constant, (J/ mol K);** T : **Temperature, (K);** A : **Adsorption Potential, (J/mol);** P : **Equilibrium pressure, (atm);** *S model*: **Solubility normalized model;** C : **Equilibrium concentration, (mg/L);** *DA Model*: **Dubinin Astakhov isotherm Model;** A : **Adsorption Potential from S/ C model, (J/ mol);** E : **Distribution co-efficient of adsorption energy;** n : **Distribution parameter of heterogenous surface**

Data Availability All the data are available and can be provided to the editorial team on request.

Declarations

Ethical Approval The authors declare that ethical considerations have been taken care of while writing the manuscript.

Consent to Participate The review paper does not involve human subjects.

Consent to Publish We declare that there is no conflict of interest associated with this manuscript. As the corresponding author, we confirm that the manuscript has been proofread and approved for submission by all named authors.

Ms. Amrutha
Dr. Chikmagalur Raju Girish (corresponding author)
Dr. Gautham Jeppu (corresponding author)
Dr. Balakrishna Prabhu
Ms. Katharina Mayer

Competing Interests The authors declare that there is no conflict of interest associated with this work, and the manuscript has been approved for submission by all named authors.

References

Abbas Q, Yousaf B, Amina Ali MU, Munir MAM, El-Naggar A, Rinklebe J, Naushad M (2020) Transformation pathways and fate of engineered nanoparticles (ENPs) in distinct interactive environmental compartments: A review. Environ Int 138:105646. https://doi.org/10.1016/j.envint.2020.105646

Abdoul Magid ASI, Islam MS, Chen Y, Weng L, Sun Y, Chang X, Zhou B, Ma J, Li Y (2021) Competitive adsorption of Dibutyl phthalate (DBP) and Di(2-ethylhexyl) phthalate (DEHP) onto fresh and oxidized corncob biochar. Chemosphere 280. https://doi.org/10.1016/j.chemosphere.2021.130639

Acosta-Herrera AA, Hernández-Montoya V, Castillo-Borja F, Pérez-Cruz MA, Montes-Morán MA, Cervantes FJ (2021) Competitive adsorption of pollutants from anodizing wastewaters to promote water reuse. J Environm Manag 293. https://doi.org/10.1016/j.jenvman.2021.112877

Adamu H, Shand M, Taylor RSF, Manyar HG, Anderson JA (2018) Use of carbon-based composites to enhance performance of TiO2 for the simultaneous removal of nitrates and organics from aqueous environments. Environ Sci Pollut Res 25(32):32001–32014. https://doi.org/10.1007/s11356-018-3120-x

Ahechti M, Benomar M, El Alami M, Mendiguchía C (2022) Metal adsorption by microplastics in aquatic environments under controlled conditions: exposure time, pH and salinity. Int J Environ Anal Chem 102(5):1118–1125. https://doi.org/10.1080/03067319.2020.1733546

Al-Asheh S, Banat F, Al-Omari R, Duvnjak Z (2000) Predictions of binary sorption isotherms for the sorption of heavy metals by pine bark using single isotherm data. Chemosphere 41(5):659–665. https://doi.org/10.1016/S0045-6535(99)00497-X

Al-Duri B (1995) A review in equilibrium in single and multicomponent liquid adsorption systems. Rev Chem Eng 11(2):101–144. https://doi.org/10.1515/REVCE.1995.11.2.101

Al-Ghouti MA, Da'ana DA (2020) Guidelines for the use and interpretation of adsorption isotherm models: A review. J Hazard Mater 393:122383. https://doi.org/10.1016/j.jhazmat.2020.122383

Al-Ghouti MA, Li J, Salamh Y, Al-Laqtah N, Walker G, Ahmad MNM (2010) Adsorption mechanisms of removing heavy metals and dyes from aqueous solution using date pits solid adsorbent. J Hazard Mater 176(1–3):510–520. https://doi.org/10.1016/j.jhazmat.2009.11.059

Arim AL, Guzzo G, Quina MJ, Gando-Ferreira LM (2018) Single and binary sorption of Cr(III) and Ni(II) onto modified pine bark. Environ Sci Pollut Res 25(28):28039–28049. https://doi.org/10.1007/s11356-018-2843-z

Babatunde KA, Negash BM, Jufar SR, Ahmed TY, Mojid MR (2022) Adsorption of gases on heterogeneous shale surfaces: A review. J Pet Sci Eng 208(2):109466. https://doi.org/10.1016/j.petrol.2021.109466

Baig KS, Doan HD, Wu J (2009) Multicomponent isotherms for biosorption of Ni^{2+} and Zn^{2+}. Desalination 249(1):429–439. https://doi.org/10.1016/j.desal.2009.06.052

Bansal RC, Goyal M (2005) Activated Carbon Adsorption (1st ed.). CRC Press pp 520. https://doi.org/10.1201/9781420028812

Roy A, Bhattacharya J (2013) A binary and ternary adsorption study of wastewater Cd(II), Ni(II) and Co(II) by c-Fe$_2$O$_3$ nanotubes. Sep Purif Technol 115:172–179. https://doi.org/10.1016/j.seppur.2013.05.010

Beyan SM, Prabhu SV, Ambio TA, Gomadurai C (2022) A statistical modeling and optimization for Cr(VI) Adsorption from aqueous media via Teff Straw-based activated carbon: isotherm, kinetics, and thermodynamic studies. Adsorpt Sci Technol. https://doi.org/10.1155/2022/7998069

Bibi S, Farooqi A, Hussain K, Haider N (2015) Evaluation of industrial based adsorbents for simultaneous removal of arsenic and fluoride from drinking water. J Clean Prod 87(1):882–896. https://doi.org/10.1016/j.jclepro.2014.09.030

Bibi S, Kamran MA, Sultana J, Farooqi A (2017) Occurrence and methods to remove arsenic and fluoride contamination in water. Environ Chem Lett 15(1):125–149. https://doi.org/10.1007/s10311-016-0590-2

Bohli T, Ouederni A, Villaescusa I (2017) Simultaneous adsorption behavior of heavy metals onto microporous olive stones activated carbon: analysis of metal interactions. Euro-Mediterr J Environ Integr 2(1):1–15. https://doi.org/10.1007/s41207-017-0030-0

Bonilla-Petriciolet A, Mendoza-Castillo DI, Reynel-Ávila HE (2017) Adsorption processes for water treatment and purification. In Adsorption Processes for Water Treatment and Purification. https://doi.org/10.1007/978-3-319-58136-1

Choy KKH, Porter JF, Mckay G (2004) Intraparticle diffusion in single and multicomponent acid dye adsorption from wastewater onto carbon. Chem Eng J 103(1–3):133–145. https://doi.org/10.1016/j.cej.2004.05.012

Cobbina SJ, Duwiejuah AB, Quainoo AK (2019) Single and simultaneous adsorption of heavy metals onto groundnut shell biochar produced under fast and slow pyrolysis. Int J Environ Sci Technol 16(7):3081–3090. https://doi.org/10.1007/s13762-018-1910-9

Costa CSD, Queiroz BGM, Landers R, da Silva MGC, Vieira MGA (2019) Equilibrium study of binary mixture biosorption of Cr(III) and Zn(II) by dealginated seaweed waste: investigation of adsorption mechanisms using X-ray photoelectron spectroscopy analysis. Environ Sci Pollut Res 26(28):28470–28480. https://doi.org/10.1007/s11356-018-2880-7

Crittenden JC, Loper SW, Ari M, Luft P, Hand DW, Oravltz JL (1985) Prediction of multicomponent adsorption equilibria using ideal adsorbed solution theory. Environ Sci Technol 19(11):1037–1043. https://doi.org/10.1021/es00141a002

Darweesh MA, Elgendy MY, Ayad MI, Ahmed AMM, Elsayed NMK, Hammad WA (2022) Adsorption isotherm, kinetic, and optimization studies for copper (II) removal from aqueous solutions by banana leaves and derived activated carbon. S Afr J Chem Eng 40:10–20. https://doi.org/10.1016/j.sajce.2022.01.002

DhanaRamalakshmi R, Murugan M, Jeyabal V (2020) Arsenic removal using Prosopis spicigera L. wood (PsLw) carbon–iron oxide composite. Appl Water Sci 10(9). https://doi.org/10.1007/s13201-020-01298-w

Dhanasekaran P, Sahu O (2021) Arsenate and fluoride removal from groundwater by sawdust impregnated ferric hydroxide and activated alumina (SFAA). Groundw Sustain Dev 12:100490. https://doi.org/10.1016/j.gsd.2020.100490

Digiano FA, Baldauf G, Frick B, Sontheimer H (1978) A simplified competitive equilibrium adsorption model. Chem Eng Sci 33(12):1667–1673. https://doi.org/10.1016/0009-2509(78)85143-4

Ezeonuegbu BA, Machido DA, Whong CMZ, Japhet WS, Alexiou A, Elazab ST, Qusty N, Yaro CA, Batiha GES (2021) Agricultural waste of sugarcane bagasse as efficient adsorbent for lead and nickel removal from untreated wastewater: Biosorption, equilibrium isotherms, kinetics and desorption studies. Biotechnol Rep 30:e00614. https://doi.org/10.1016/j.btre.2021.e00614

Febrianto J, Kosasih AN, Sunarso J, Ju YH, Indraswati N, Ismadji S (2009) Equilibrium and kinetic studies in adsorption of heavy metals using biosorbent: A summary of recent studies. J Hazard Mater 162(2–3):616–645. https://doi.org/10.1016/j.jhazmat.2008.06.042

Field NJ (2017) Investigation of multicomponent adsorption isotherms in chromatography using high-throughput formats, Doctoral dissertation, The Advanced Centre for Biochemical Engineering, Department of Biochemical Engineering, University College London, pp 368. http://discovery.ucl.ac.uk/id/eprint/10054098/1/Nick%20Field%20final%20thesis.pdf. Accessed 15-3-2023

Foo KY, Hameed BH (2010) Insights into the modeling of adsorption isotherm systems. Chem Eng J 156(1):2–10. https://doi.org/10.1016/j.cej.2009.09.013

Fornstedt T (2010) Characterization of adsorption processes in analytical liquid – solid chromatography 1217:792–812. https://doi.org/10.1016/j.chroma.2009.12.044

Fritz W, Merk W, Schlünder EU (1981) Competitive adsorption of two dissolved organics onto activated carbon-II. Adsorption kinetics in batch reactors. Chem Eng Sci 36(4):743–757. https://doi.org/10.1016/0009-2509(81)85089-0

Giraldo J, Nassar NN, Benjumea P, Pereira-Almao P, Cortés FB (2013) Modeling and prediction of asphaltene adsorption isotherms using Polanyi's modified theory. Energy Fuels 27(6):2908–2914. https://doi.org/10.1021/ef4000837

Girish CR (2018) Simultaneous adsorption of pollutants onto the adsorbent review of interaction mechanism between the pollutants and the adsorbent. Int J Eng Technol (UAE) 7(4):3613–3622. https://doi.org/10.14419/ijet.v7i4.19671

Girish CR (2019) Various isotherm models for multicomponent adsorption: A review. Int J Civil Eng Technol (IJCIET) 8(10):80–86

Girish CR, Murty VR (2016) Mass transfer studies on adsorption of phenol from wastewater using Lantana camara, Forest Waste. Int J Chem Eng. https://doi.org/10.1155/2016/5809505

González-López ME, Laureano-Anzaldo CM, Pérez-Fonseca AA, Arellano M, Robledo-Ortíz JR (2022) A critical overview of adsorption models linearization: methodological and statistical inconsistencies. Sep Purif Rev 51(3):358–372. https://doi.org/10.1080/15422119.2021.1951757

Guibal RSVE, Beppu EASMM (2007) Adsorption and desorption of binary mixtures of copper and mercury ions on natural and crosslinked chitosan membranes: 603–611. https://doi.org/10.1007/s10450-007-9050-4

Gun'ko VM (2007) Competitive adsorption. Theoret Exp Chem 43(3):139–183. https://doi.org/10.1007/s11237-007-0020-4

He J, Yang Y, Wu Z, Xie C, Zhang K, Kong L, Liu J (2020) Review of fluoride removal from water environment by adsorption. In Journal of Environmental Chemical Engineering (Vol. 8, Issue 6) Elsevier B.V. https://doi.org/10.1016/j.jece.2020.104516

Istratie R, Stoia M, Păcurariu C, Locovei C (2019) Single and simultaneous adsorption of methyl orange and phenol onto magnetic iron oxide/carbon nanocomposites. Arab J Chem 12(8):3704–3722. https://doi.org/10.1016/j.arabjc.2015.12.012

Jadhav AJ, Srivastava VC (2019) Multicomponent adsorption isotherm modeling using thermodynamically inconsistent and consistent models. AIChE J 65(11). https://doi.org/10.1002/aic.16727

Janani R, Gurunathan B, K S, Varjani S, Ngo HH, Gnansounou E (2022) Advancements in heavy metals removal from effluents employing nano-adsorbents: Way towards cleaner production. Environ Res 203:111815. https://doi.org/10.1016/j.envres.2021.111815

Jeppu GP, Clement TP (2012) A modified Langmuir-Freundlich isotherm model for simulating pH-dependent adsorption effects. J Contam Hydrol 129–130:46–53. https://doi.org/10.1016/j.jconhyd.2011.12.001

Jeppu GP, Clement TP, Lee K, Barnett MO (2010) A scalable surface complexation modeling framework for predicting arsenate adsorption on goethite-coated sands 27(2). https://doi.org/10.1089/ees.2009.0045

Khan AR, Ataullah R, Al-Haddad A (1997) Equilibrium adsorption studies of some aromatic pollutants from dilute aqueous solutions on activated carbon at different temperatures. J Colloid Interf Sci 194(1):154–165. https://doi.org/10.1006/jcis.1997.5041

Kondor A, Santmarti A, Mautner A, Williams D, Bismarck A, Lee K-Y (2021) On the BET surface area of nanocellulose determined using volumetric, gravimetric and chromatographic adsorption methods. Front Chem Eng 3:1–12. https://doi.org/10.3389/fceng.2021.738995

Kong Q, Preis S, Li L, Luo P, Wei C, Li Z, Hu Y, Wei C (2020) Relations between metal ion characteristics and adsorption performance of graphene oxide: A comprehensive experimental and theoretical study. Sep Purif Technol 232:115956. https://doi.org/10.1016/j.seppur.2019.115956

Kurniawati D, Bahrizal, Sari TK, Adella F, Sy S (2021) Effect of contact time adsorption of Rhodamine B, Methyl orange and methylene blue colours on langsat shell with batch methods. J Phys: Conf Ser 1788(1). https://doi.org/10.1088/1742-6596/1788/1/012008

Lakherwal D (2019) Adsorption of heavy metals-a review. Int J Environ Sci Dev4(1):41–48

Lee CKM, Stenstrom MK (1996) Competitive Adsorption of Cyclotrimethylenetrinitramine (RDX) and Cyclotetramethylenetetranitramine (HMX), Department of Civil and Environmental Engineering University of California, Los Angeles, California, School of Engineering and Applied Science Report No. ENG 96-152. http://www.seas.ucla.edu/stenstro/r/r39.pdf. Accessed 15-3-2023

Chen WS, Chen YC, Lee CH (2022a) Modified activated carbon for copper ion removal from aqueous solution. Processes 10(1). https://doi.org/10.3390/pr10010150

Chen X, Hossain MF, Duan C, Lu J, Tsang YF, Islam MS, Zhou Y (2022b) Isotherm models for adsorption of heavy metals from water - A review. Chemosphere 307(P1):135545. https://doi.org/10.1016/j.chemosphere.2022.135545

Li YH, Ding J, Luan Z, Di Z, Zhu Y, Xu C, Wu D, Wei B (2003) Competitive adsorption of Pb2+, Cu2+ and Cd 2+ ions from aqueous solutions by multiwalled carbon nanotubes. Carbon 41(14):2787–2792. https://doi.org/10.1016/S0008-6223(03)00392-0

Malvar JL, Martín J, del Mar Orta M, Medina-Carrasco S, Santos JL, Aparicio I, Alonso E (2020) Simultaneous and individual adsorption of ibuprofen metabolites by a modified montmorillonite. Appl Clay Sci 189:105529. https://doi.org/10.1016/j.clay.2020.105529

Manning BA, Goldberg S (1996) Modeling competitive adsorption of arsenate with phosphate and Molybdate on oxide minerals. Soil Sci Soc Am J 60(1):121–131. https://doi.org/10.2136/sssaj1996.03615995006000010020x

McKay G, Al-Duri B (1991) Extended empirical Freundlich isotherm for binary systems: a modified procedure to obtain the correlative constants. Chem Eng Process 29(3):133–138. https://doi.org/10.1016/0255-2701(91)85012-D

Mohan D, Singh KP (2002) Single- and multi-component adsorption of cadmium and zinc using activated carbon derived from bagasse - An agricultural waste. Water Res 36(9):2304–2318. https://doi.org/10.1016/S0043-1354(01)00447-X

Mukhtar A, Saqib S, Safdar F, Hameed A, Rafiq S, Mellon NB, Amen R, Khan MS, Ullah S, Assiri MA, Babar M, Bustam MA, Rehman WU, Merican ZMA (2020) Experimental and comparative theoretical study of thermal conductivity of MWCNTs-kapok seed oil-based nanofluid. Int Commun Heat Mass Transfer 110. https://doi.org/10.1016/j.icheatmasstransfer.2019.104402

Musso TB, Parolo ME, Pettinari G (2019) pH, ionic strength, and ion competition effect on Cu(II) and Ni(II) sorption by a Na-bentonite used as liner material. Pol J Environ Stud 28(4):2299–2310. https://doi.org/10.15244/pjoes/84922

Mustafa S, Irshad M, Waseem M, Shah KH, Rashid U, Rehman W (2013) Adsorption of heavy metal ions in ternary systems onto Fe(OH)3. Korean J Chem Eng 30(12):2235–2240. https://doi.org/10.1007/s11814-013-0178-5

Noroozi B, Sorial GA (2013) Applicable models for multi-component adsorption of dyes: A review. J Environ Sci (China) 25(3):419–429. https://doi.org/10.1016/S1001-0742(12)60194-6

Padilla-Ortega E, Leyva-Ramos R, Flores-Cano JV (2013) Binary adsorption of heavy metals from aqueous solution onto natural clays. Chem Eng J 225:535–546. https://doi.org/10.1016/j.cej.2013.04.011

Pereira SK, Kini S, Prabhu B, Jeppu GP (2023) A simplified modeling procedure for adsorption at varying pH conditions using the modified Langmuir-Freundlich isotherm. Appl Water Sci 13(1):1–13. https://doi.org/10.1007/s13201-022-01800-6

Piplai T, Kumar A, Alappat BJ (2018) Removal of ZnO and CuO nanoparticles from water using an activated carbon column. J Environ Eng 144(3):04017113. https://doi.org/10.1061/(asce)ee.1943-7870.0001331

Puri N, Gupta A, Mishra A (2021) Recent advances on nano-adsorbents and nanomembranes for the remediation of water. J Clean Prod 322:129051. https://doi.org/10.1016/j.jclepro.2021.129051

Qiao J, Cui Z, Sun Y, Hu Q, Guan X (2014) Simultaneous removal of arsenate and fluoride from water by Al-Fe (hydr)oxides. Front Environ Sci Eng 8(2):169–179. https://doi.org/10.1007/s11783-013-0533-0

Qiao S, Hu X (2000) Role of pore size distribution in the binary adsorption kinetics of gases in activated carbon. Stud Surf Sci Catal 128:401–410. https://doi.org/10.1016/s0167-2991(00)80045-2

Qu J, Tian X, Jiang Z, Cao B, Akindolie MS, Hu Q, Feng C, Feng X, Meng X, Zhang Y (2020) Multi-component adsorption of Pb(II), Cd(II) and Ni(II) onto microwave-functionalized cellulose: Kinetics, isotherms, thermodynamics, mechanisms and application for electroplating wastewater purification. J Hazard Mater 387. https://doi.org/10.1016/j.jhazmat.2019.121718

Radke CJ, Prausnitz JM (1972) Thermodynamics of multi-solute adsorption from dilute liquid solutions. AIChE J 18(4):761–768. https://doi.org/10.1002/aic.690180417

Ramesh ST, Rameshbabu N, Gandhimathi R, Nidheesh PV, Srikanth Kumar M (2012) Kinetics and equilibrium studies for the removal of heavy metals in both single and binary systems using hydroxyapatite. Appl Water Sci 2(3):187–197. https://doi.org/10.1007/s13201-012-0036-3

Rathore VK, Dohare DK, Mondal P (2016) Competitive adsorption between arsenic and fluoride from binary mixture on chemically treated laterite. J Environ Chem Eng 4(2):2417–2430. https://doi.org/10.1016/j.jece.2016.04.017

Ashour M, Alprol AE, Khedawy M, Abualnaja KM, Mansour AT (2022) Equilibrium and kinetic modeling of crystal violet dye adsorption by a marine Diatom, Skeletonema costatum. Materials 15(18). https://doi.org/10.3390/ma15186375

Russell SM, Carta G (2005) Multicomponent protein adsorption in supported cationic polyacrylamide hydrogels. AIChE J 51(9):2469–2480. https://doi.org/10.1002/aic.10482

Sağ Y, Açikel Ü, Aksu Z, Kutsal T (1998) A comparative study for the simultaneous biosorption of Cr(VI) and Fe(III) on C. vulgaris and R. arrhizus: Application of the competitive adsorption models. Process Biochem 33(3):273–281. https://doi.org/10.1016/S0032-9592(97)00060-5

Saikia MD, Dutta NN (2008) Adsorption affinity of certain biomolecules onto polymeric resins: Effect of solute chemical nature. React Funct Polym 68(1):33–38. https://doi.org/10.1016/j.reactfunctpolym.2007.10.013

Say R, Yilmaz N, Denizli A (2003) Biosorption of cadmium, lead, mercury, and arsenic ions by the fungus Penicillium purpurogenum. Sep Sci Technol 38(9):2039–2053. https://doi.org/10.1081/SS-120020133

Sellaoui L, Soetaredjo FE, Ismadji S, Bonilla-Petriciolet A, Belver C, Bedia J, Ben Lamine A, Erto A (2018) Insights on the statistical physics modeling of the adsorption of Cd2+ and Pb2+ ions on bentonite-chitosan composite in single and binary systems. Chem Eng J 354:569–576. https://doi.org/10.1016/j.cej.2018.08.073

Sheng PX, Ting YP, Chen JP (2007) Biosorption of heavy metal ions (Pb, Cu, and Cd) from aqueous solutions by the Marine Alga Sargassum sp. in single- And multiple-metal systems. Ind Eng Chem Res 46(8):2438–2444. https://doi.org/10.1021/ie0615786

Sohn S, Kim D (2005) Modification of Langmuir isotherm in solution systems — definition and utilization of concentration dependent factor 58:115–123. https://doi.org/10.1016/j.chemosphere.2004.08.091

Srivastava SK, Tyagi R (1995) Competitive adsorption of substituted phenols by activated carbon developed from the fertilizer waste slurry. Water Res 29(2):483–488. https://doi.org/10.1016/0043-1354(94)00182-7

Srivastava VC, Mall ID, Mishra IM (2008) Removal of cadmium(II) and zinc(II) metal ions from binary aqueous solution by rice husk ash. Colloids Surf A 312(2–3):172–184. https://doi.org/10.1016/j.colsurfa.2007.06.048

Stoeckli F (1998) Recent developments in Dubinin's theory. Carbon 36(4):363–368. https://doi.org/10.1016/S0008-6223(97)00194-2

Sun X, Huang H, Zhu Y, Du Y, Yao L, Jiang X, Gao P (2019) Adsorption of Pb^{2+} and Cd^{2+} onto Spirulina platensis harvested by polyacrylamide in single and binary solution systems. Colloids Surf A Physicochem Eng Aspects 583:123926. https://doi.org/10.1016/j.colsurfa.2019.123926

Tien C (2019) Fixed-bed adsorption models and fixed-bed design calculations. In Introduction to Adsorption. https://doi.org/10.1016/b978-0-12-816446-4.00006-3

Van Assche TRC, Baron GV, Denayer JFM (2018) An explicit multicomponent adsorption isotherm model: accounting for the size-effect for components with Langmuir adsorption behavior. Adsorption 24(6):517–530. https://doi.org/10.1007/s10450-018-9962-1

Wang F, Pan Y, Cai P, Guo T, Xiao H (2017) Single and binary adsorption of heavy metal ions from aqueous solutions using sugarcane cellulose-based adsorbent. Biores Technol 241:482–490. https://doi.org/10.1016/j.biortech.2017.05.162

Wang J, Guo X (2020) Adsorption isotherm models: Classification, physical meaning, application and solving method. Chemosphere 258:127279. https://doi.org/10.1016/j.chemosphere.2020.127279

Weerasundara L, Ok YS, Bundschuh J (2021) Selective removal of arsenic in water: A critical review. Environ Pollut 268:115668. https://doi.org/10.1016/j.envpol.2020.115668

Wu D, Hu Z, Wang X, He S, Kong H (2007) Use of zeolitized coal fly ash in the simultaneous removal of ammonium and phosphate from aqueous solution. Front Environ Sci Eng China 1(2):213–220. https://doi.org/10.1007/s11783-007-0037-x

Wu Y, Jiang L, Wen YJ, Zhou JX, Feng S (2012) Biosorption of Basic Violet 5BN and Basic Green by waste brewery's yeast from single and multicomponent systems. Environ Sci Pollut Res 19(2):510–521. https://doi.org/10.1007/s11356-011-0577-2

Yang RT (2003) Adsorbents : fundamentals and applications. John Wiley & Sons

Yazdani M, Mahmoodi NM, Arami M, Bahrami H (2012) Surfactant-Modified Feldspar : Isotherm , Kinetic , and Thermodynamic of Binary System Dye Removal 14:1–10. https://doi.org/10.1002/app

Zhang Y, Liu L, Zhang P, Wang J, Xu M, Deng Q, Zeng Z, Deng S (2019) Ultra-high surface area and nitrogen-rich porous carbons prepared by a low-temperature activation method with superior gas selective adsorption and outstanding supercapacitance performance. Chem Eng J 355:309–319. https://doi.org/10.1016/j.cej.2018.08.169

Zhou X (2020) Correction to the calculation of Polanyi potential from Dubinnin-Rudushkevich equation. J Hazard Mater 384:121101. https://doi.org/10.1016/j.jhazmat.2019.121101

Zhu J, Katti AM, Guiochon G (1991) Comparison of various isotherm models for predicting competitive adsorption data. J Chromatogr A 552(C):71–89. https://doi.org/10.1016/S0021-9673(01)95924-2